Chronic NGF treatment induces somatic hyperexcitability in cultured dorsal root ganglion neurons of the rat

(NGF 処置したラット背根神経節ニューロンの興奮性亢進)

The United Graduate School of Veterinary Science

Yamaguchi University

Tomohiko KAYANO

March 2014

CONTENTS

INTRODUCTION

Pain is a vital function of the nervous system in providing the body with a warning of potential or actual injury. In some case, peripheral nerve damages, e.g., diseases and traumas, frequently results in neuropathic pain. The most important symptoms are chronic pain, abnormal sensations to painful (hyperalgesia) and painless (allodynia) stimuli. Neuropathic pain is less responsive and sometimes refractory to conventional analgesic treatment, including non-steroidal anti-inflammatory drugs (NSAIDs) and opioid derivatives (Chen et al., 2004; Namaka et al., 2004).

Experimental peripheral nerve injury induces neuropathic symptoms (Wall et al., 1979; Bennett and Xie, 1988; Seltzer et al., 1990; Kim and Chung, 1992; Decosterd and Woolf, 2000; Winkelstein et al., 2001). Although primary sensory neurons of healthy animals are “silent” in electrophysiology without excitatory inputs from other neurons or sensational inputs, abnormal spontaneous firing was observed in sensory neurons of animals with nerve injury (Kajander and Bennett, 1992; Kajander et al., 1992; Devor et al., 1994; Matzner and Devor, 1994). Therefore, this abnormal firing is considered to be a cause of neuropathic pain. However, neither the pathogenic mechanisms of hyperexcitability nor the mechanisms triggering spontaneous firings in DRG neurons remain clear.

Nerve growth factor (NGF) was identified originally as a survival factor for sensory and sympathetic neurons in the developing nervous system (Levi-Montalcini and Angeletti, 1968; Ritter et al., 1991). In adult, NGF is not required for survival, but it has a crucial role in the generation of acute and chronic pain (Levi-Montalcini et al., 1996; Pezet and McMahon, 2006). For example, intrathecal administration of NGF applied in adult rats has been reported to result in hyperalgesia (Lewin et al., 1993). The NGF concentration in DRG was reported to increase after the artificial nerve injury (Herzberg et al., 1997; Shen et al., 1999). Animals shown that heat heyperalgesia can be abolished by concurrent administration of anti-NGF (Lewin et al., 1992). These reports suggest that NGF correlates with the pathogenesis of neuropathic pain.

NGF binds to two types of receptor on DRG neurons: the low-affinity receptor, $p75^{NTR}$ (Casaccia-Bonnefil et al., 1999) and the high-affinity receptor, tyrosine kinase A (trkA) (Barbacid, 1994), through which NGF exerts its main influence on sensory neurons (Wiesmann and de Vos, 2001). Not only TrkA but also $p75^{NTR}$ is expressed in a subgroup of DRG neurons that is assumed to be nociceptive (Lawson et al., 1997; Lawson et al., 2002). Immunoreactivity for both NGF receptors was observed in the part of cultured DRG neurons in our preparation (Kitamura et al., 2005).

Kitamura et al. reported that more than 20 % DRG neurons that are isolated from

healthy adult rats and cultured in the presence of NGF longer than 3 days showed spontaneous spikes (Kitamura et al., 2005). These spontaneous spikes were abolished by tetrodotoxin and lidocaine, the voltage-gated Na^+ channel blockers, and reduction of extracellular Na^+ concentration from 154 mM to 100 mM, in all-or-none fashion, suggesting that spontaneous current spikes reflected spontaneous action potentials (APs). From these results, it became evident that DRG neurons of adult rats had a nature to respond to NGF and obtained the abnormal hyperexcitability to fire spontaneously.

However, it is questioned how the somatic hyperexcitablity to fire spontaneously is composed, and where the triggering sources of the spontaneous firing exist in the NGF-treated DRG neurons. In results section I, to know underlying mechanisms triggering the spontaneous discharges of the NGF-treated DRG neurons in culture, the voltage clamp and current clamp recording in the whole-cell and outside-out configurations was made. Moreover, although it is evident that chronic treatment of NGF induced the spontaneous APs of DRG neurons in cell culture, it is not clear that what types of DRG neurons are affected by NGF. Ozaki et al. previously reported that fluctuation of intracellular Ca^{2+} concentration ($[Ca^{2+}]_i$) evoked by spontaneous APs was observed in small and medium sized NGF-treated DRG neurons and in capsaicin-sensitive neurons more frequently than in capsaicin-non-responsive neurons

(Ozaki et al., 2009).

Nociceptors are generally part of the small and medium diameter DRG population and respond to noxious mechanical stimuli and heat (Lawson et al., 1993; Hoheisel et al., 1994). In addition, these sensory fibers also respond to chemical stimuli (Julius and Basbaum, 2001). Thus, nociceptors are considered polymodal. The activation of specific receptors or ion channels underlies the transduction of noxious stimuli into APs at peripheral nociceptive nerve terminals (Millan, 1999). TRP channels have been found in many cell types, including sensory neurons. TRP channels play important roles in pain sensation because they serve as molecular sensors that detect variety of stimuli (Patapoutian et al., 2003). Indeed, TRP channels are related to specific sensations, such as mechanosensation, thermosensation and pain (Montell, 2001; Minke and Cook, 2002). A large family of TRP channels has been identified (Ramsey et al., 2006). We focused on the three thermally sensitive TRP channels, TRPV1, TRPA1 and TRPM8. They are activated by >43 ºC, <25 ºC, and <17 ºC, respectively (Patapoutian et al., 2009). They can also be activated by the exogenous ligands, capsaicin (TRPV1), menthol (TRPM8), and icilin (TRPM8 and TRPA1) (Caterina et al., 1997; McKemy et al., 2002b; Peier et al., 2002). Moreover, they are expressed in DRG neurons (Kobayashi et al., 2005) and are thought to be the main TRP ion channels involved in

pain sensation. It is also reported that TRPA1, but not TRPM8, is expressed together with TRPV1 in the same neurons; it is suggested that such neurons are expected to have physiological roles not simply as thermo sensors, but also as nociceptors (McKemy et al., 2002a; Story et al., 2003; Babes et al., 2004; Kobayashi et al., 2005). In section II, therefore, in order to investigate that the profile of the subpopulations of DRG neurons that becomes hyperexcitable due to NGF, we investigated them by observing the $[Ca^{2+}]_i$ responses to capsaicin and icilin.

MATERIALS AND METHODS

Cell isolation and culture

DRG neurons were isolated from adult male Sprague-Dawley rats or Wistar rats (7-12 weeks old), using procedures reported previously (Komagiri and Kitamura, 2003; Kitamura et al., 2005; Ozaki et al., 2009). Rats were killed by cervical dislocation after diethyl ether inhalation anesthesia. Animals were sacrificed according to the guidelines stipulated by the ethical committee of Tottori University. Ganglia were dissected from the entire length of the vertebral column (Fig. 1). Axons extending from the ganglia were removed as much as possible under a stereoscopic microscope. The ganglia were incubated at 37 ˚C in Ca^{2+}-Mg^{2+}-free phosphate-buffered saline (PBS) containing collagenase type IV (500 U/ml, Worthington Biochemicals, Lakewood, NJ, USA), DNase I (0.12 μg/ml, Sigma, St Louis, MO, USA) and BSA (1 mg/ml, Sigma) for 2 h, then rinsed with PBS to remove the collagenase. The ganglia were then incubated in PBS containing trypsin (0.25% w/v, Invitrogen, Carlsbad, CA, USA) and BSA (1 mg/ml) for 15 min. After the enzymatic digestion, the cells were gently triturated with a silicon-coated Pasteur pipette and centrifuged at 500 × g for 5 min to remove the enzymes. The isolated cells were suspended in DMEM (Invitrogen) containing 4.5 g/l of glucose and cultured on coverslips coated with poly-D-lysine (Sigma). The cells were

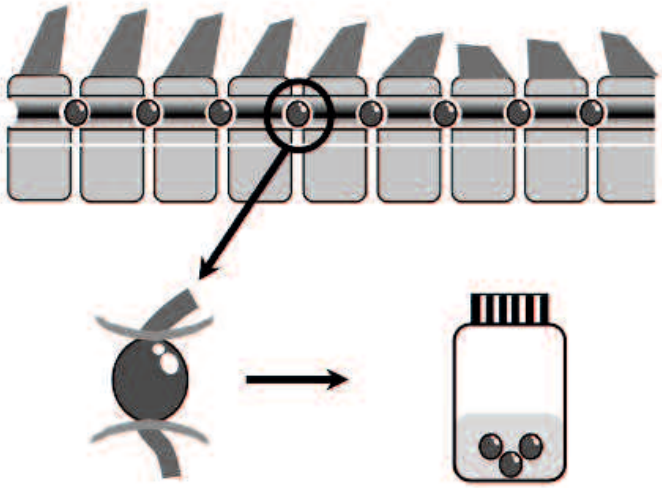

Fig. 1. An outline of DRG neurons isolation. Rat ganglia were dissected from entire length of the vertebral column. Axons extending from ganglia were removed under the stereoscopic microscope and incubated in calcium-magnesium free phosphate-buffered saline containing collagenase type IV or trypsin (see material and methods).

kept at 37 ˚C in a humidified atmosphere of 95 % air and 5 % CO_2 and cultured until use. DMEM was supplemented with 10 % FBS (MP Biochemicals, Irvine, CA, USA), 100 U/ml of penicillin (Invitrogen), 100 ng/ml of streptomycin (Invitrogen), and 10-μM cytosine–β–arabinoside (Sigma). The culture medium was changed every 2 days. NGF-7S (100 ng/ml, Sigma) was added to the medium 2 days after plating. Patch clamp recordings and $[Ca^{2+}]_i$ measurements were performed from the 4th to the 14th day of culture. Neurons that were cultured for more than 2 days in the presence of NGF were considered as NGF-treated neurons.

Electrophysiology

The cell-attach patch, whole-cell and outside-out patch recordings were made at room temperature (22 - 24 ˚C). Heat-polished glass electrodes with a 2.5- to 4-MΩ tip resistance were used. DRG neurons with a small diameter (10-30 μm) that had been reported to mainly include C-neurons in vivo (Harper and Lawson, 1985) were used to record membrane potential and current (Fig. 2). The normal bath solution consisted of (in mM): 144 NaCl, 10 NaOH, 6 KCl, 1.2 $MgCl_2$, 2.5 $CaCl_2$, 10 D-glucose and 10 HEPES (Sigma), and pH was adjusted to 7.4 with HCl. In order to adjust the concentration of Na^+ exactly, we used HCl to adjust pH. The Na^+-reduced solution was

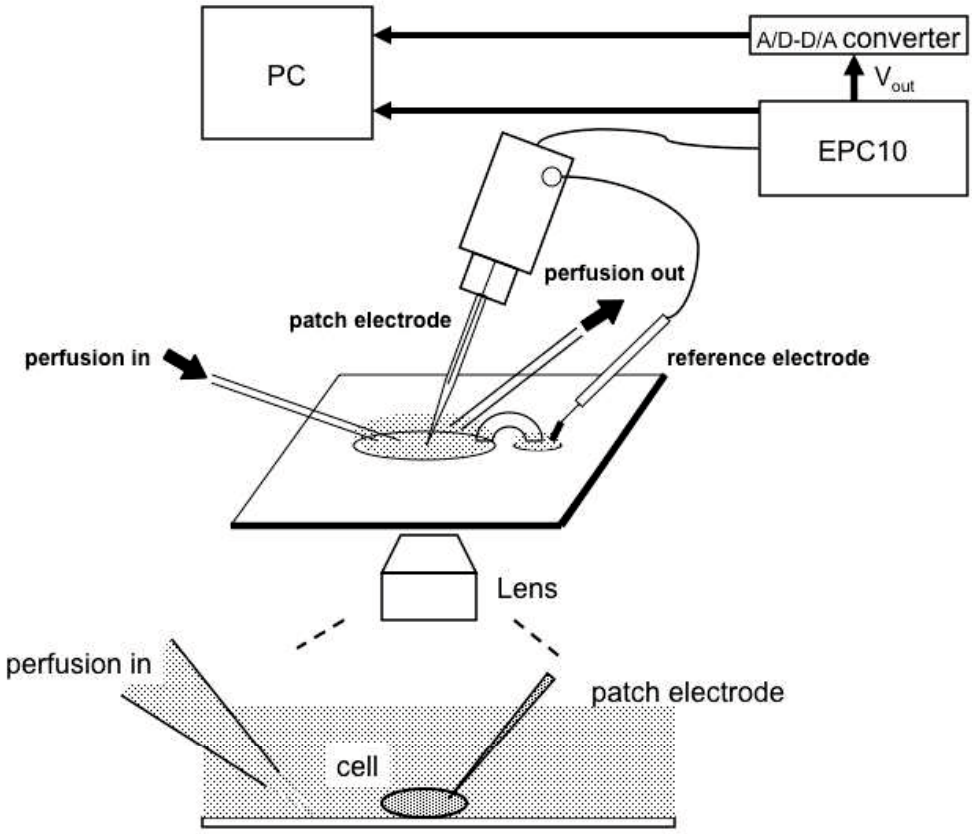

Fig. 2. The experimental setup using the EPC-10 patch-clamp amplifier and HEKA pulse software (see materials and methods).

made by the isotonic replacement of Na^+ with N-methyl-D-glucamine$^+$ ($NMDG^+$, Merck, Darmstadt, Germany). The Ca^{2+}-free solution was made by removing $CaCl_2$ and increasing the concentration of $MgCl_2$ to 5 mM. The pipette solution consisted of (in mM): 151.6 K-methansulfonic acid, 3.4 KCl, 5 Na-methansulfonic acid, 2 $MgCl_2$, 1.3 $CaCl_2$, 10 EGTA (Sigma) and 10 HEPES, and pH was adjusted at 7.3 with methansulfonic acid. The liquid junction potential between the pipette solution and the bath solution (approximately −10 mV) was corrected. Neurons were continuously perfused with the bath solution at a flow rate of 1 ml/min throughout the experiments. Currents and potentials were measured with a patch-clamp amplifier (CEZ-2400, Nihon Koden, Tokyo, Japan or EPC-10, HEKA, Germany). Cell capacitances were determined by integrating area under a capacity transient current elicited by a −10 mV voltage step from the holding potential and a series resistance (Rs) was also calculated from the capacity transient and the cell capacitance. Voltage errors at the holding potential caused by Rs were less than 1 mV, and were not corrected. In some neurons, after the whole-cell recording, the voltage clamp recording in the outside-out configuration was made. The outside-out patch membranes were excised by gently taking off the pipette tip from the neuronal membranes. The tip of the pipette was placed farther than 5 mm from the soma during recording. Under this recording condition, there were no visible

membrane structures connected to the original neuron, such as cytoplasmic tubes.

Data acquisition was performed at a sampling frequency of 40 kHz throughout the experiments by a personal computer (Macintosh, Apple, Cupertino, CA, USA) in conjunction with an analog/digital converter (Power Lab, AD Instruments, Castle Hill, NSW, Australia). Data were analyzed with Lab Chart (AD Instruments), Patch Master (HEKA), IGOR Pro (Wavemetrics, Lake Oswego, OR, USA) and Excel (Microsoft, Redmond, WA, USA). Data are presented as mean values ± SEM (n = the number of observations). Statistical significance was assessed by Student's *t*-test. Differences were considered statistically significant if $P < 0.05$.

$[Ca^{2+}]_i$ measurement

$[Ca^{2+}]_i$ in cultured rat DRG neurons was measured with the fluorescent Ca^{2+} indicator Fura-2, according to a procedure reported previously (Ozaki et al., 2009). Cultured neurons attached to round coverslips (11 mm in diameter) were incubated in HEPES-buffered normal solution (in mM: 144 NaCl, 10 NaOH, 6 KCl, 2 $CaCl_2$, 5 $MgCl_2$, 10 Glucose, 10 HEPES, pH 7.4 adjusted with HCl; the concentration of Na^+ was fixed at 154 mM) containing Fura-2/AM (3 μM, Merck, Whitehouse Station, NJ, USA) for 60 min at room temperature (22 - 24 ºC). After the incubation, a coverslip was

mounted in a chamber fixed on the stage of an inverted fluorescence microscope (IX71, Olympus, Tokyo, Japan). Neurons were continuously perfused with various experimental solutions through polyethylene tubes connected to a peristaltic pump (Minipulse 3, Gilson, Middleton, WI, USA) at a flow rate of 1.4 ml/min (*Fig. 3*). In this system, the solution around the neurons could be changed rapidly within a few seconds. Changes in $[Ca^{2+}]_i$ were measured by dual excitation microfluorometry using a digital image analyzer (Aqua Cosmos/Ratio, Hamamatsu Photonics, Hamamatsu, Japan). The fluorescent signal was detected using a UV objective lens (UApo 20×3/340, Olympus), and the emission, passed through a band pass filter (500 ± 10 nm), was detected by a cooled CCD camera (ORCA-ER, Hamamatsu Photonics). All experiments were performed at room temperature (22 - 24 ºC).

Data acquisition was performed using a procedure reported previously (Ozaki et al., 2009). Briefly, data were obtained at a sampling frequency of 0.2 Hz using Aqua Cosmos software (Hamamatsu Photonics). The fluorescent intensity at the excitation wavelengths of 340 (F340) and 380 nm (F380) was determined by the analyzing software (Aqua Cosmos, Hamamatsu Photonics). To calculate $[Ca^{2+}]_i$ in individual neurons, regions of interest (ROIs) were chosen to include the soma of each DRG neuron, and the average values of $[Ca^{2+}]_i$ in all pixels contained in each ROI were

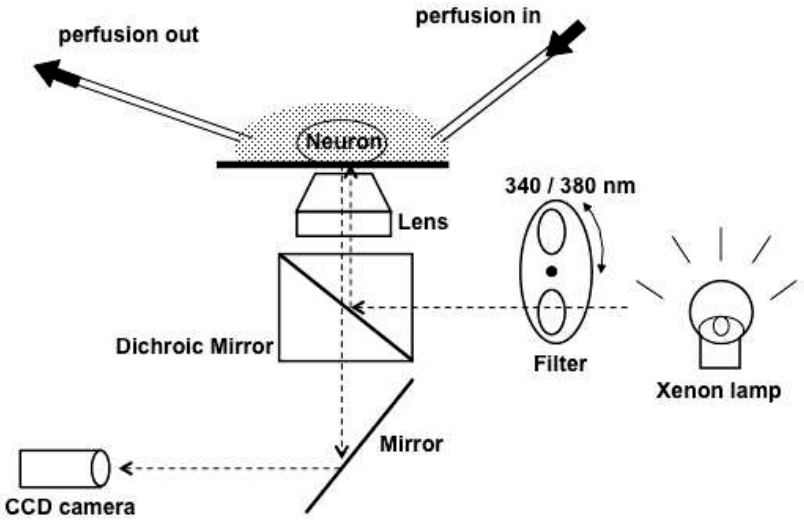

Fig. 3. An outline of dual excitation microfluorometry. The cells were excited at two wavelengths of light (340 nm and 380 nm) alternately. For each second, one 340/380 ratio was obtained. The ratio between emitted fluorescence intensities of 340 nm and 380nm signals were calculated by Aqua Cosmos/Ratio. The corresponding $[Ca^{2+}]_i$ increase was elucidated from the calibration data (see materials and methods).

calculated. Changes in the calculated $[Ca^{2+}]_i$ were analyzed by Igor Pro (Wavemetrics, Lake Oswego, OR, USA) and Excel (Microsoft, Redmond, WA, USA). The degree of spontaneous $[Ca^{2+}]_i$ fluctuations was quantitatively assessed according to an analytical procedure reported previously (Ozaki et al., 2009). Data are presented as the means ± S.E.M. The statistical significance was assessed by Student's *T*-test and the analysis of variance (ANOVA). Differences were considered statistically significant if $p < 0.05$.

Solutions and Drugs

A concentrated stock solution of NGF-7S at 10 μg/ml was made in DMEM and stored at −30 ˚C until use. Na-methansulfonic acid and K-methansulfonic acid were made from NaOH and KOH by mixing methansulfonic (Wako Pure Chemicals) acid at 1:1, respectively. A concentrated stock solution of TTX at 1 mM was made in a citrate-buffered solution and stored at −30 ºC until use. A solution containing 100 mM Na^+ was made isotonic with N-methyl-D-glucamine$^+$ ($NMDG^+$). Similarly, a solution containing high K^+ (60 mM) was made by the isotonic replacement of Na^+ with K^+. A Ca^{2+}-free solution was made by simply omitting $CaCl_2$ from the normal solution. As voltage-gated Ca^{2+} channel (VGCC) blockers, nifedipine at 1 μM, SNX-482 at 0.2 μM, ω-agatoxin IVA at 0.1 μM and ω-conotoxin GVIA at 1 μM were used against L-type,

R-type, P/Q-type and N-type channels, respectively. A concentrated stock solution of nifedipine was made in DMSO at 0.1 mM and stored at –30 ˚C until use. Concentrated stock solutions of SNX-482, ω-agatoxin IVA and ω-conotoxin GVIA were made in D.W. and stored at –30 ˚C until use. Concentrated stock solutions of icilin (Sigma), capsaicin (Sigma) at 100 mM and cyclopiazonic acid (CPA, Sigma) at 10 mM were made in DMSO and stored at –30 ˚C until use. All other chemicals used were of an analytical grade.

RESULTS : I

Spontaneous current spikes in NGF-treated DRG neurons

Rat DRG neurons cultured in the absence and presence of NGF (100 ng/ml) were used for the patch clamp recording. After establishing a giga ohm seal, the cell-attached recording was made. Figures 4A and B show typical traces of current responses recorded from the neurons cultured in the absence (A) and presence of NGF for 2 days (B), respectively. In the control neuron, only a stable holding current with a stable noise of about 20 pA was observed (A). On the other hand, spontaneous current spikes were observed in the some populations of the NGF-treated neuron as shown in B. An expanded current trace of a typical spontaneous event is shown in Fig. 4C. Previously we have reported that such spontaneous current spikes in the cell-attached configuration reflect the APs (Kitamura et al., 2005). In this study, the whole-cell recording in the voltage clamp mode was made after the cell-attached recording. Figures 4D and E show current traces after the membrane rupture in the same neurons as shown in Fig. 4A and B, respectively. In the control neuron, a stable holding current with no spontaneous event was observed at a holding potential of −50 mV (Fig. 4D). In contrast, spontaneously occurring current spikes, named here "I_{sp}", were recorded in the neuron cultured with NGF (Fig. 4E). Two examples of expanded traces of I_{sp} are shown in Fig.

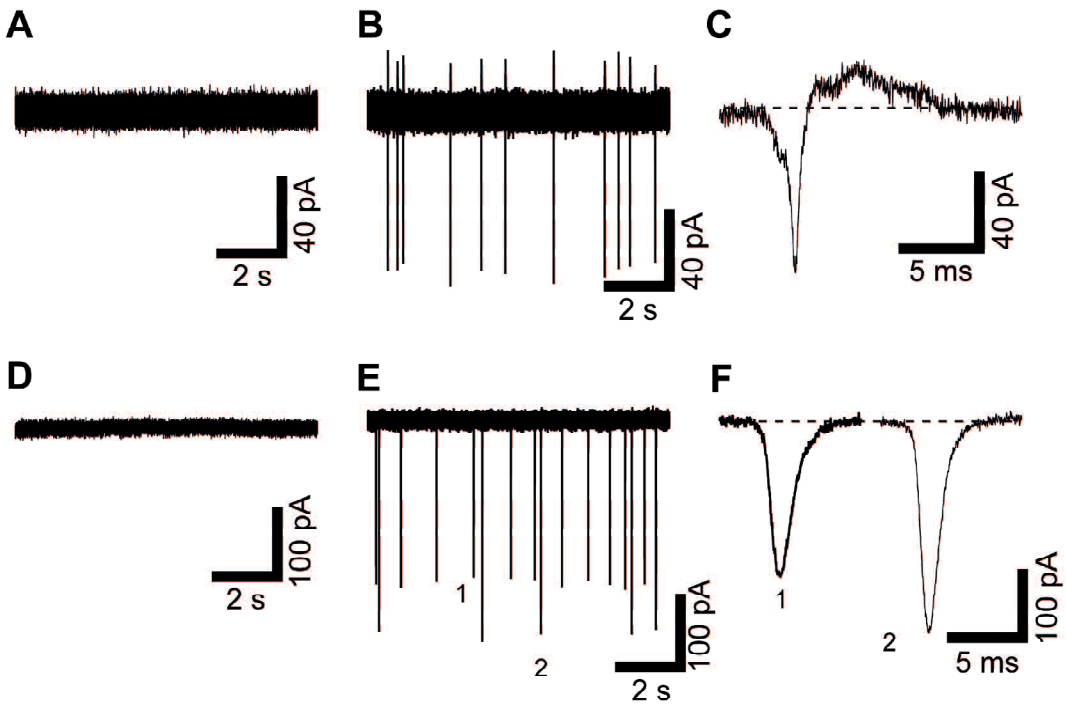

Fig. 4. NGF-treated DRG neurons with on-cell firings show spontaneously generated transient inward current spikes in the whole-cell voltage clamp configuration. (A, B) Cell-attached recording under the voltage-clamped condition at 0 mV in neurons cultured in the absence (A) or presence (B) of NGF. (C) A time-expanded trace of a representative current event in B. The dotted line represents a holding current level of the neuron. (D, E) Whole-cell recording under the voltage-clamped condition at –50 mV. The neurons in D and E were identical to those in A and B, respectively. Spontaneous inward current spikes (I_{sp}) were observed in the neuron presented in E. (F) Time-expanded traces of I_{sp} numbered in E.

4F. In order to examine a correlation between spontaneous firing in the cell-attached configuration (on-cell firing) and I_{sp} in the whole-cell configuration, the proportions of the number of the neurons showing I_{sp} among all tested neurons with and without the on-cell firing were calculated. In this analysis, results from neurons cultured in the presence and absence of NGF were combined. In 673 neurons showing no spontaneous on-cell firing, only 29 neurons showed I_{sp} (4.3%). In 150 neurons showing spontaneous on-cell firing, I_{sp} were observed in 113 neurons (75.3%).

In the neuron shown in Fig. 4E, two kinds of I_{sp} with two different amplitudes were observed. Another typical current trace including I_{sp} from the neuron cultured for 3 days with NGF is shown in Fig. 5A. From this neuron, three kinds of I_{sp} with clearly different amplitudes were recorded. Expanded traces of three typical I_{sp} (numbered 1-3) are shown in Fig. 5B. Each I_{sp} had a transient inward current followed by a small transient outward current. Among all tested neurons whose membrane capacitance was 25.4 ± 1.9 pF (n = 66), inward amplitudes of I_{sp} varied from –27 pA to –2.5 nA and the averaged amplitude of I_{sp} at –50 mV was –315 ± 36 pA. The frequency of I_{sp} also varied among neurons: I_{sp} was observed once every 30 seconds in one neuron, and more than 5 times a second in another. On the other hand, kinetics of I_{sp} were relatively stable among tested neurons. Width time at 20%, 50% and 80% of the peak amplitude of the inward current

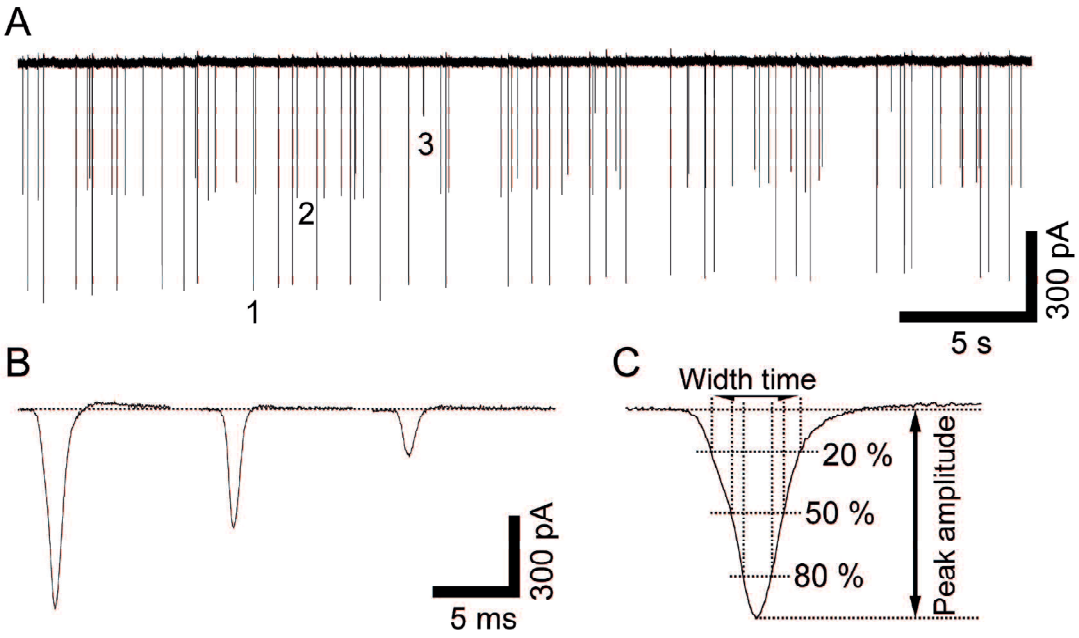

Fig. 5. Analysis scheme of kinetics of I_{sp}. (A) Another typical trace of I_{sp} at –50 mV in the whole-cell mode. (B) Time-expanded traces of I_{sp} numbered in A. (C) Analysis scheme of I_{sp} kinetics. Width time of each I_{sp} at 10, 20, 50 and 80% level is assessed in this study.

was assessed to quantify the kinetics of I_{sp} in the subsequent analysis (Fig. 5C). The mean values of width time at 20%, 50% and 80% of I_{sp} 23 independent neurons were 3.63 ± 0.36 ms, 2.08 ± 0.20 ms and 1.07 ± 0.07 ms, respectively.

Na^+ is a charge-carrying ion of I_{sp}

Since calculated reversal potential (E_{rev}) for Na^+, Ca^{2+} and K^+ in the whole-cell configuration was +88, +160 and –83 mV, respectively, inward component of I_{sp} at –50 mV was expected to result from an increase in the conductance for Na^+ and/or Ca^{2+}, and/or decrease in the K^+ conductance. To examine what ions carry the inward component of I_{sp}, I_{sp} were recorded at various holding potentials between –70 to –30 mV. Typical traces (A) and summarized data (B) are shown in Fig. 6. Superimposed and expanded I_{sp} traces at different holding potentials in the same neuron as that shown in A are drawn in C. Since two different amplitudes of I_{sp} were recorded at each potential, traces of I_{sp} with the larger amplitude were drawn. The kinetics of I_{sp} were not affected by the change in the holding potential, but the amplitude of I_{sp} significantly increased with increase in the negative holding potential. This result suggested that the decrease in the conductance for K^+ did not contribute to the generation of I_{sp}. Therefore, it was expected that the increase in the conductance for Ca^{2+} and/or Na^+ contributed to

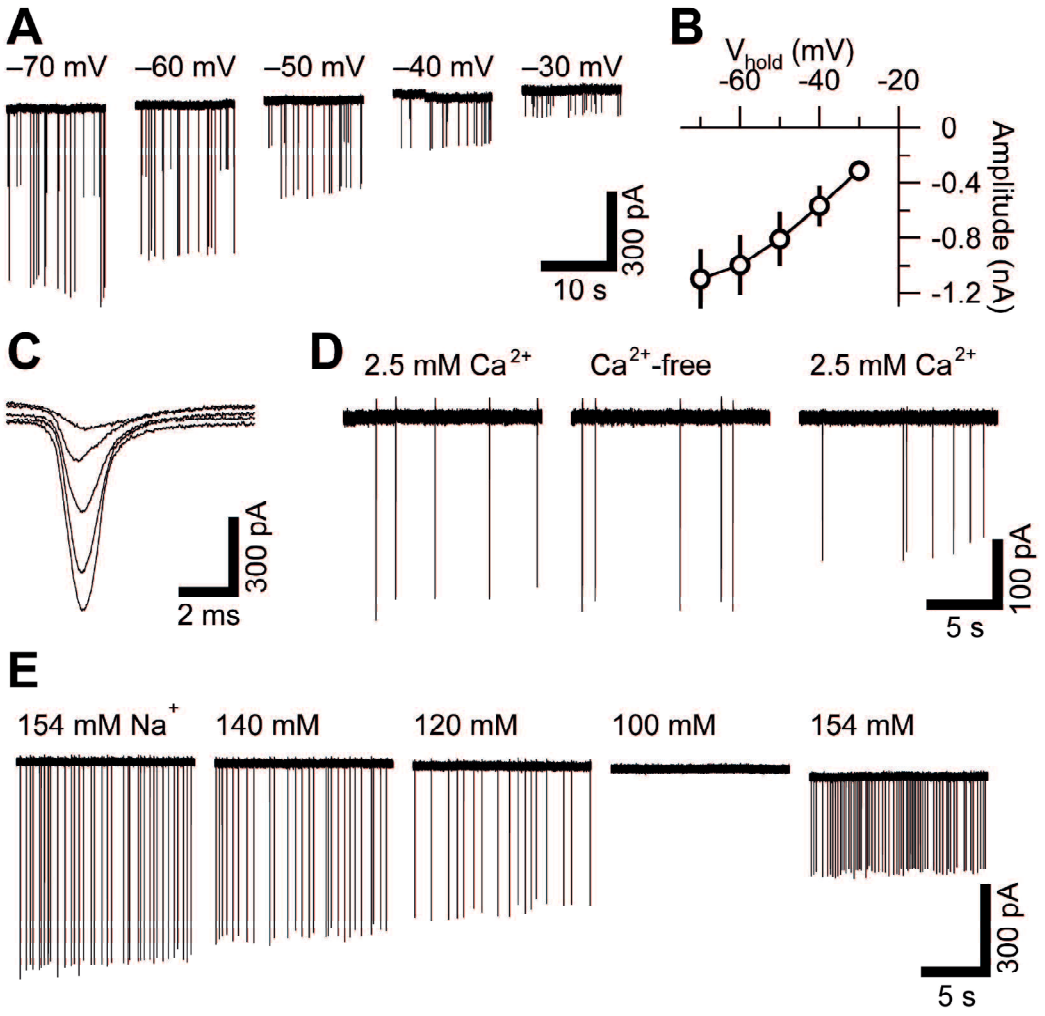

Fig. 6. Determination of charge carrying ions of I_{sp}. (A) Typical traces of I_{sp} in one neuron voltage-clamped at various holding potentials. (B) Mean amplitudes and SEM of I_{sp} at each holding potential in 6 independent neurons are plotted against the holding potentials. Typical values in each neuron at each holding potential are calculated from more than 20 I_{sp} observed continuously. (C) Time-expanded traces of typical I_{sp} at each holding potential in A. (D) Traces of I_{sp} in a neuron before, during and after exposure to Ca^{2+}-free solution. (E) Solutions with decreasing concentrations of extracellular Na^{+} were applied to I_{sp}-generating neuron. The neuron was perfused with solutions at each Na^{+} concentration for 1 min.

I_{sp}. To confirm this point, effects of decrease in extracellular Ca^{2+} and Na^{+} concentrations on the amplitude of I_{sp} at –50 mV were examined. As shown in Fig. 6D, removal of extracellular Ca^{2+} did not show significant effects on the I_{sp} amplitudes (n = 10), suggesting Ca^{2+} was not a main charge-carrying ion of I_{sp}. When extracellular Na^{+} concentrations were gradually decreased, I_{sp} suddenly disappeared in the presence of 100-mM Na^{+} in an "all-or-none" fashion in the neuron shown in Fig. 6E. The Na^{+} reduction to 120 mM abolished I_{sp} in 2 of 9 tested neurons, and, that to 100 mM abolished I_{sp} in the remaining 7 neurons. Reintroduction of Na^{+} to 154 mM restored the I_{sp} in all tested neurons. The calculated E_{rev} for Na^{+} in the presence of 154, 120 and, 100 mM of extracellular Na^{+} was +88, +81 and, +77 mV, respectively. When the concentration of Na^{+} decreased from 154 mM to 100 mM, the inward driving force of Na^{+} decreased only 9.2% at –50 mV. Similar results were obtained when Na^{+} was replaced with $Tris^{+}$ or $choline^{+}$ instead of $NMDG^{+}$.

I_{sp} reflects the action potential

It is well known that compartments that cannot be voltage-clamped sufficiently exist in a voltage-clamped cell in the whole-cell configuration. Axons and/or dendrites extending from the soma are candidates for such a compartment. The all-or-none

blocking action of Na^+ reduction on I_{sp} suggests a hypothesis that spontaneous discharges like APs occurred in such unclamped compartments and resulted in I_{sp}. A depolarizing phase of the discharge might reflect the inward component of I_{sp}, and an afterhyperpolarization, the outward component. To examine this hypothesis, we examined effects of the voltage-gated Na^+ channel (VGSCs) blockers, tetrodotoxin (TTX) and lidocaine on I_{sp}. Increasing concentrations of TTX (0.1 to 100 nM, Fig. 7A) and lidocaine (1 to 1000 μM, Fig. 7B) were applied to the NGF-treated neurons. In the neuron shown in Fig. 7A, in the presence of TTX at the concentrations below 10 nM, I_{sp} was observed. Although their frequency tended to decrease by TTX, the amplitude was similar to that of the control. However, in the presence of 100-nM TTX, I_{sp} disappeared in an all-or-none fashion. Similar results were obtained in the seven other neurons: I_{sp} was abolished by 0.1-nM TTX in 1 neuron, by 10-nM in 2 neurons, and by 100-nM in 5 neurons. Lidocaine similarly blocked I_{sp} in an all-or-none fashion (Fig. 7B). I_{sp} was abolished by lidocaine at 100 μM in 1 of 6 neurons and at 1 mM in the other 5 neurons. These results indicate that the activation of VGSCs, i.e. regenerative discharges, resulted in I_{sp}.

Since repolarization in the AP results from an activation of voltage-gated K^+ channels, an effect of a cocktail of K^+ channel blockers: TEA (3 mM), 4-AP (2 mM)

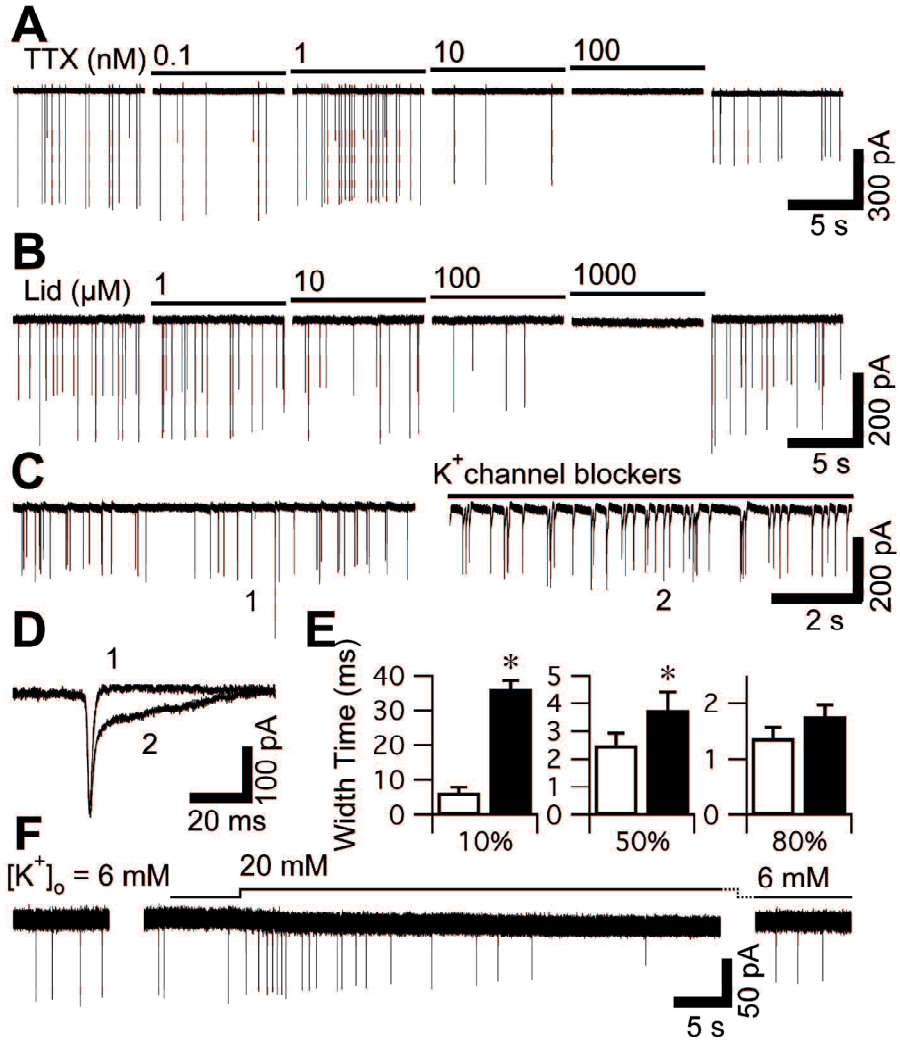

Fig. 7. I_{sp} reflects spontaneous discharges generated in the loosely voltage-clamped membrane regions. (A, B) Increasing concentrations of TTX (A) and lidocaine (B) were applied to I_{sp}-generating neurons held at –50 mV. Each concentration of TTX and lidocaine were applied for 30 s. After the washing out of the blockers, I_{sp} recovered. (C) I_{sp} at –50 mV before, during and after exposure to a cocktail of K^+ channel blocking agents. TEA (3 mM), 4-AP (2 mM) and $BaCl_2$ (0.5 mM) were applied in combination for 2 min. (D) Time-expanded traces of I_{sp} numbered in C are superimposed. (E) Summarized data on width time at the 10%, 50% and 80% level of I_{sp} before (open columns) and during (closed columns) exposure of the neurons to the K^+ channel blocking agents. Columns and vertical bars indicate the mean ± SEM in 5 independent neurons. (F) A typical trace of I_{sp} at –50 mV in the presence of 20-mM extracellular K^+. The neuron was exposed to a 20 mM K^+-containing solution for 1 min. *: $p < 0.05$ with the paired Student's *t*-test.

and $BaCl_2$ (0.5 mM) on I_{sp} were examined. This cocktail inhibited completely the depolarization-induced outward K^+ currents in the whole-cell voltage-clamped DRG neurons used in this study (data not shown). Although I_{sp} were observed in the presence of K^+ channel blockers, the kinetics of I_{sp} were quite different from that before the exposure (Fig. 7C). In the presence of K^+ channel blockers, the recovery of I_{sp} to the baseline was clearly slower (Fig. 7D). The parameters of I_{sp} kinetics were assessed similarly as indicated in Fig. 6C (Fig. 7E). The blockade of the voltage-gated K^+ channels significantly prolonged the width time at 10% and 50% of the amplitudes, supporting the hypothesis that I_{sp} reflected the spontaneous discharges.

Assuming that the spontaneous discharges occurred in loosely voltage-clamped regions of cell membranes, the membrane potential in those regions should be affected by the extracellular concentration of K^+. To confirm this point, effects of the higher concentration of K^+ on I_{sp} were examined (Fig. 7F). In neurons showing I_{sp}, when the concentration of extracellular K^+ was raised from 6 to 20 mM, the amplitude and the frequency of I_{sp} were gradually decreased, the inward holding current slightly increased, and finally I_{sp} disappeared. This blocking effect was reversible: After the concentration of K^+ returned to 6 mM, I_{sp} reappeared. Similar results were obtained in the other 7 neurons.

Multiple amplitudes of I_{sp} in one neuron

As shown in Fig. 4 to 7, in many neurons multiple types of I_{sp} with different amplitudes were recorded in the individual neurons. Another typical trace of whole-cell I_{sp} with two different amplitudes is shown in Fig. 8A and some traces of I_{sp} are expanded in B. In this neuron, I_{sp} consisting of twin peaks (for example event #1) was observed. In the other case, two different I_{sp} occurred with no interval (event #4). I_{sp} with multiple peaks was rarely observed in neurons showing I_{sp} at low frequency (less than 1 Hz), but was often observed in neurons with I_{sp} at higher frequency. Each I_{sp} with twin peaks has usually different amplitudes of peaks, each of which has similar amplitudes to I_{sp} with a single peak in the same neuron. Amplitudes of I_{sp} and the area under each I_{sp} were plotted against the recording time in Fig. 8C and D, respectively. The amplitude and the area of each type of I_{sp} were stable throughout the recording. The area under the I_{sp} with twin peaks (e.g. event #1 and 4, open triangles) and the largest I_{sp} (event #5, closed triangles) was equal to the sum of the amplitudes of two different types of I_{sp}, suggesting that two types of I_{sp} in this neuron occurred independently. Similar results were obtained in all the 7 neurons analyzed.

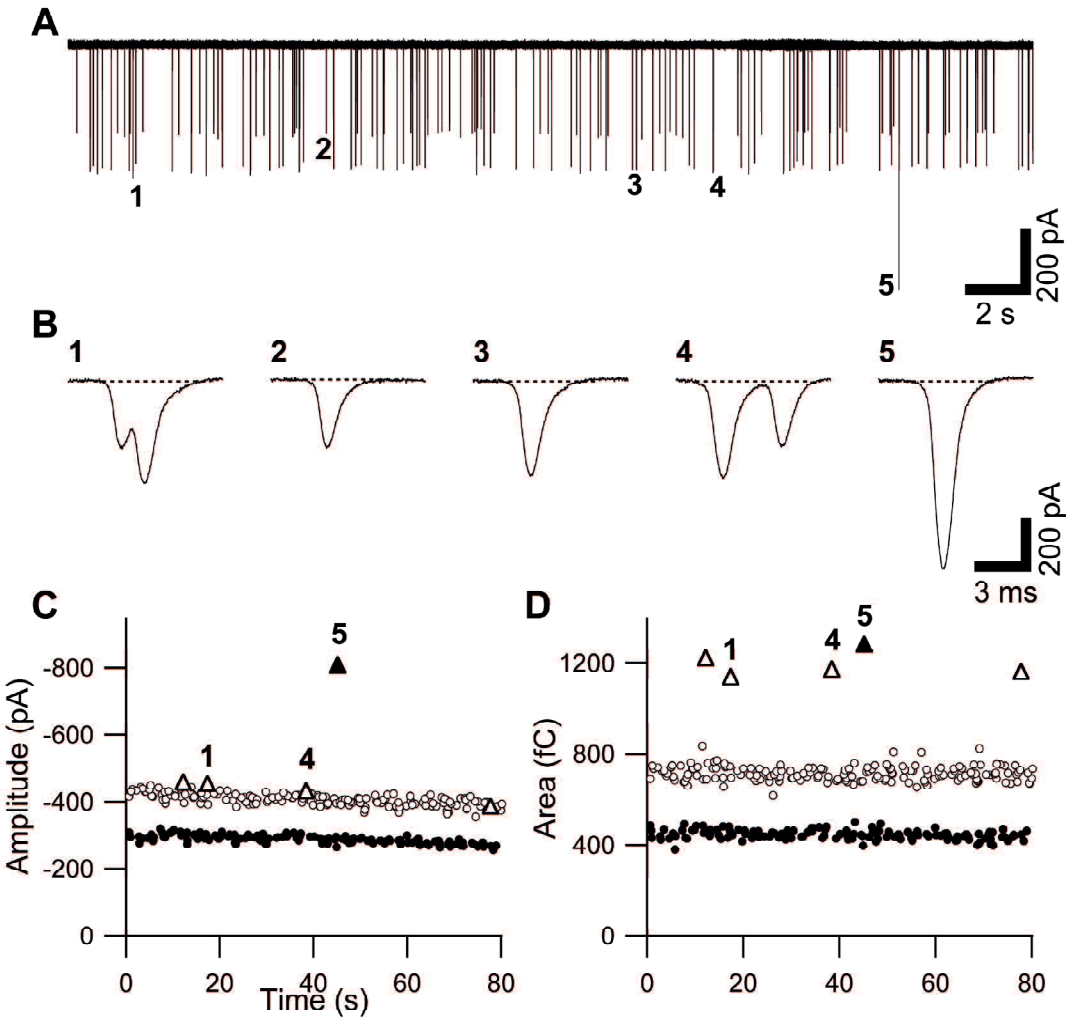

Fig. 8. Multiple types of I_{sp} with different amplitudes occur in the single neuron. (A) Whole-cell recording under the voltage-clamped condition at –50 mV. (B) Time-expanded traces of I_{sp} numbered 1-5 in A. (C, D) Peak amplitude of I_{sp} (C) and Area under each I_{sp} (D) are plotted against time. The solid circles (e.g. numbered 2 in B) and the open circles (e.g. numbered 3 in B) and the solid triangle (numbered 5 in B) indicate those of I_{sp} with a single peak. The open triangles indicate those of I_{sp} with twin peaks (e.g. 1 and 4 in B).

I_{sp} observed in excised outside-out patch

After a series of I_{sp} was recorded in the whole-cell configuration, patch membranes were excised and currents in the outside-out configuration were recorded at the holding potential of −50 mV. In 15 outside-out patch membranes excised from neurons showing I_{sp} in the whole-cell configuration, a spontaneously and transiently activated inward macroscopic current was observed. In the neuron presented in Fig. 9A, I_{sp} with two clearly different amplitudes were observed in the whole-cell configuration, while spikes with a single stable amplitude were observed in the outside-out configuration. Figure 9B shows the expanded and overlaid traces of the typical I_{sp}, numbered 1-3 in A. The kinetics of each current spike were analyzed as indicated in Fig. 5C. Data on 10 neurons showing large enough I_{sp} in the outside-out patches to analyze their amplitudes and durations are presented in Table 1 and Fig. 9C. The ratio of I_{sp} amplitudes in the outside-out configuration to that in the whole-cell configuration in each neuron varied from 0 (means no outside-out currents) to approximately 0.3 (#2 and #6 neurons in Table 1). On average, the amplitude of I_{sp} in the outside-out patch configuration was about one tenth of that in the whole-cell configuration. On the other hand, the width time of I_{sp} was similar between the whole-cell I_{sp} and the outside-out I_{sp}. The duration of I_{sp} in the outside-out patch membrane was slightly shorter than that of whole-cell

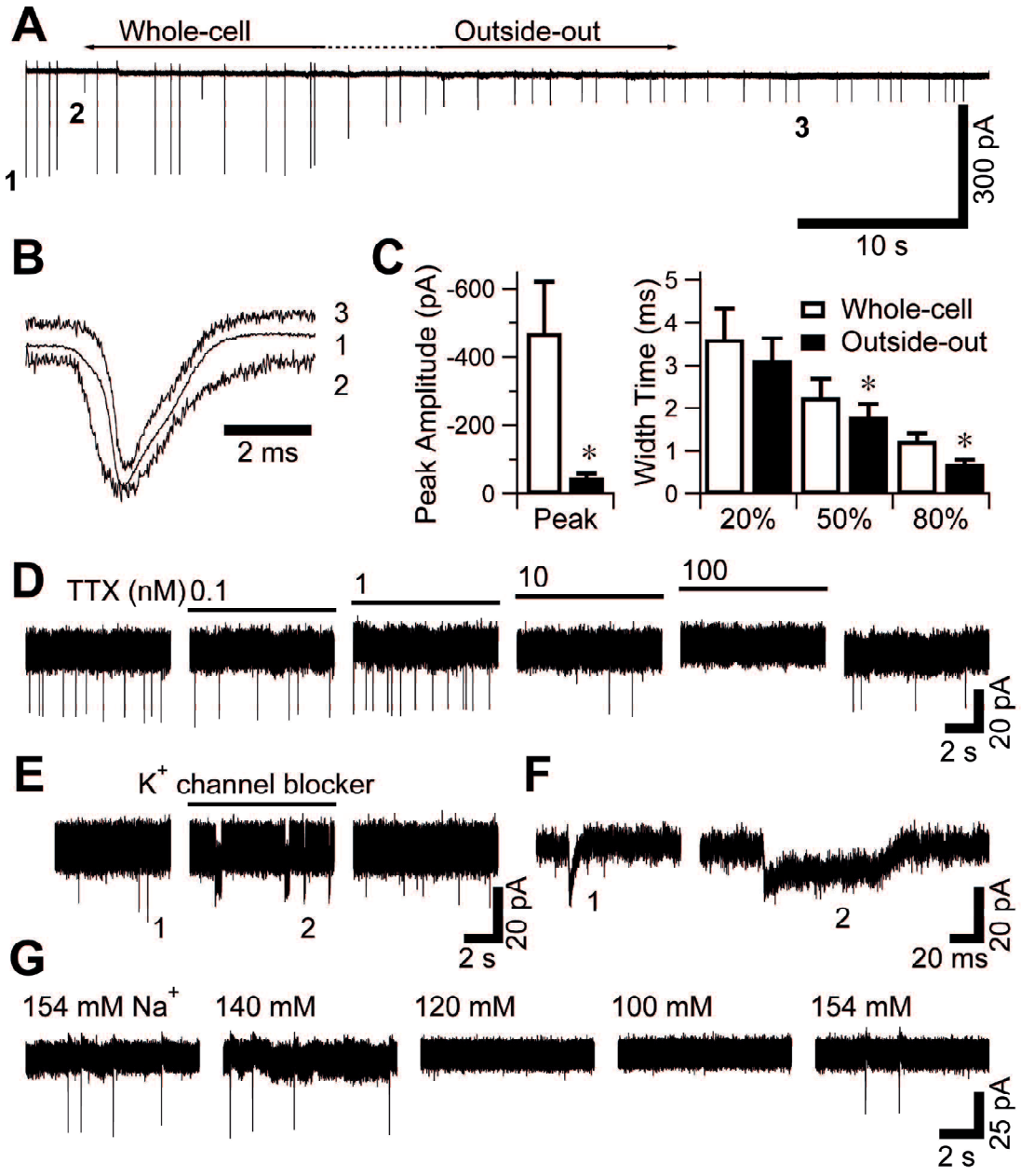
A
Whole-cell
Outside-out
1
2
3
300 pA
10 s
B
3
1
2
2 ms
C
Peak Amplitude (pA)
-600
-400
-200
0
Peak
*
Width Time (ms)
5
4
3
2
1
0
Whole-cell
Outside-out
*
*
20%
50%
80%
D
TTX (nM) 0.1
1
10
100
2 s
20 pA
E
K+ channel blocker
1
2
2 s
20 pA
F
1
2
20 ms
20 pA
G
154 mM Na+
140 mM
120 mM
100 mM
154 mM
2 s
25 pA

Fig. 9. Macroscopic I_{sp} in excised outside-out patch membranes. (A) Continuous recording before, during and after excision of a patch membrane from the whole-cell configuration to the outside-out configuration. The holding potential was –50 mV. (B) Time- and amplitude- expanded traces of I_{sp} numbered 1 to 3 in A are superimposed. (C) Means and SEM of peak amplitudes (left plot) and width time at 20%, 50% and 80% (right plot) in the whole-cell (open columns) and the outside-out (closed columns) configurations from 10 neurons held at –50 mV. The mean values in each neuron are identical to those in Table 1. *: $P < 0.05$ with the paired Student's *t*-test. (D) Increasing concentrations of TTX were applied to the I_{sp}-generating outside-out patch membrane held at –50 mV. TTX at each concentration was applied for 30 s. After the washing out of TTX, I_{sp} recovered. (E) I_{sp} recorded in the excised outside-out patch held at –50 mV before, during and after exposure to the cocktail of K^+ channel blocking agents. TEA (3 mM), 4-AP (2 mM) and $BaCl_2$ (0.5 mM) were applied in combination for 2 min. (F) Time-expanded traces of I_{sp} numbered in E. (G) Solutions with decreasing concentrations of extracellular Na^+ were applied to the I_{sp}-generating outside-out patch membrane held at –50 mV. The excised patch membrane was perfused with solutions at each Na^+ concentration for 1 min.

Table 1. Comparison of I_{sp} parameters between the whole-cell and outside-out configurations.

Whole-cell configuration

Neuron#	Amplitude	Width time (ms)			n
	(pA)	20%	50%	80%	
#1	-406 ± 45	2.61 ± 0.18	1.72 ± 0.09	1.04 ± 0.04	28
#2	-217 ± 22	3.81 ± 0.14	2.37 ± 0.08	1.34 ±0.04	42
#3	-247 ± 5	3.14 ± 0.07	2.03 ± 0.04	1.25 ± 0.03	12
#4	-205 ± 3	9.49 ± 0.08	5.79 ± 0.06	2.64 ± 0.06	26
#5	-186 ± 14	3.32 ± 0.04	2.07 ± 0.03	1.19 ± 0.02	27
#6	-427 ± 37	3.58 ± 0.07	2.28 ± 0.05	1.24 ± 0.04	62
#7	-662 ± 26	2.22 ± 0.02	1.35 ± 0.01	0.80 ± 0.01	115
#8	-440 ± 2	2.44 ± 0.01	1.47 ± 0.01	0.88 ± 0.01	22
#9	-235 ± 23	3.45 ± 0.09	2.24 ± 0.07	1.26 ± 0.04	36
#10	-1676 ± 81	2.15 ± 0.03	1.21 ± 0.01	0.73 ± 0.01	21

Outside-out configuration

Neuron#	Amplitude	Width time (ms)			n
	(pA)	20%	50%	80%	
#1	-44 ± 4**	2.89 ± 0.09	1.72 ± 0.04	0.85 ± 0.02*	21
#2	-63 ± 3**	2.83 ± 0.04**	1.68 ± 0.02**	0.96 ± 0.01**	28
#3	-26 ± 5**	2.96 ± 0.43	1.29 ± 0.43	0.23 ± 0.14**	16
#4	-47 ± 3**	6.98 ± 0.09**	4.23 ± 0.08**	1.31 ± 0.12**	25
#5	-40 ± 3**	3.32 ± 0.10	1.77 ± 0.05**	0.49 ± 0.08**	22
#6	-126 ± 1**	3.03 ± 0.02**	1.83 ± 0.02**	0.88 ± 0.01**	34
#7	-31 ± 3**	2.16 ± 0.08**	1.26 ± 0.04**	0.69 ± 0.03**	16
#8	-50 ± 3**	2.83 ± 0.06	1.44 ± 0.03**	0.64 ± 0.04**	32
#9	-36 ± 1**	3.19 ± 0.05**	1.99 ± 0.03**	0.59 ± 0.05**	47
#10	-21 ± 4**	1.18 ± 0.10**	0.70 ± 0.07**	0.26 ± 0.07**	13

Parameters of I_{sp} in individual neurons are presented as the mean ± SEM in both the whole-cell and outside-out configurations. *: $p < 0.05$, **: $p < 0.01$ against the corresponding values in the whole-cell configuration with Student's *t*-test.

currents at 50% and 80% level. This decrease in the duration of I_{sp} in the outside-out patch membrane may result from decrease in the S/N ratio between I_{sp} and the baseline noise. Since the kinetics of I_{sp} in the outside-out patch membrane was similar to that in the whole-cell configuration, pharmacological and ionic properties were also examined. Similarly to the whole-cell I_{sp}, the increase in the negative holding potential caused an increase in the amplitude of the outside-out macroscopic I_{sp} (data not shown). The inhibitory effect of TTX on I_{sp} was also seen in the outside-out patch membranes. In the patch membrane presented in Fig. 9D, TTX at 100 nM abolished I_{sp} completely and reversibly. Figures 9E and F showed an effect of the cocktail of TEA (3 mM), 4-AP (2 mM) and $BaCl_2$ (0.5 mM) on I_{sp} observed in the outside-out configuration. The exposure to K^+ channel blockers resulted in clear prolongation of the relaxing phase of I_{sp}. Moreover, as is observed in the whole-cell configuration, a reduction of the Na^+ concentration in the extracellular solution from 154 mM to 100 mM caused the reversible abolition of the outside-out I_{sp} in an all-or-none fashion (Fig. 9G) and the removal of extracellular Ca^{2+} had no effect on the amplitudes of I_{sp} (data not shown). All these results were reproducible in 6 neurons. The kinetics, the pharmacological properties, and the ionic properties of I_{sp} recorded in the whole-cell configuration and the outside-out configuration well resembled each other.

Spontaneous action potentials in the whole-cell current clamp mode

Typical traces of the voltage and current clamp recording in the I_{sp}-generating neuron are shown in Fig. 10A. In all I_{sp}-generating neurons, spontaneous transient depolarizing spikes were observed also in the current clamp recording. The steady resting membrane potential between spontaneous spikes was –64.0 ± 1.6 mV (n = 14). In contrast, in the neurons showing no I_{sp}, spontaneous firing was not observed also in the current clamp recording (Fig. 10B). The resting membrane potential, recorded under the current-clamped condition from NGF-treated and non-treated neurons that showed no I_{sp}, was –61.5 ± 1.9 mV (n = 16) and –62.5 ± 1.9 mV (n = 16), respectively. The resting membrane potentials among these 3 types of neurons were not different each other. In the quiescent neurons, a depolarizing current injection (c.i.) evoked an AP (Fig. 10B), indicating that the quiescent neurons had normal excitability to fire. In many hyperexcitable neurons cultured in the presence of NGF, spontaneous APs with overshoot and subthreshold small and transient depolarizing spikes were recorded in the current clamp recording (Fig. 10C). Expanded traces of the spikes numbered 1 to 4 in C are redrawn in D. Small depolarization, whose activation kinetics resembled small spikes, followed by the complete APs were observed. The small spikes may reflect

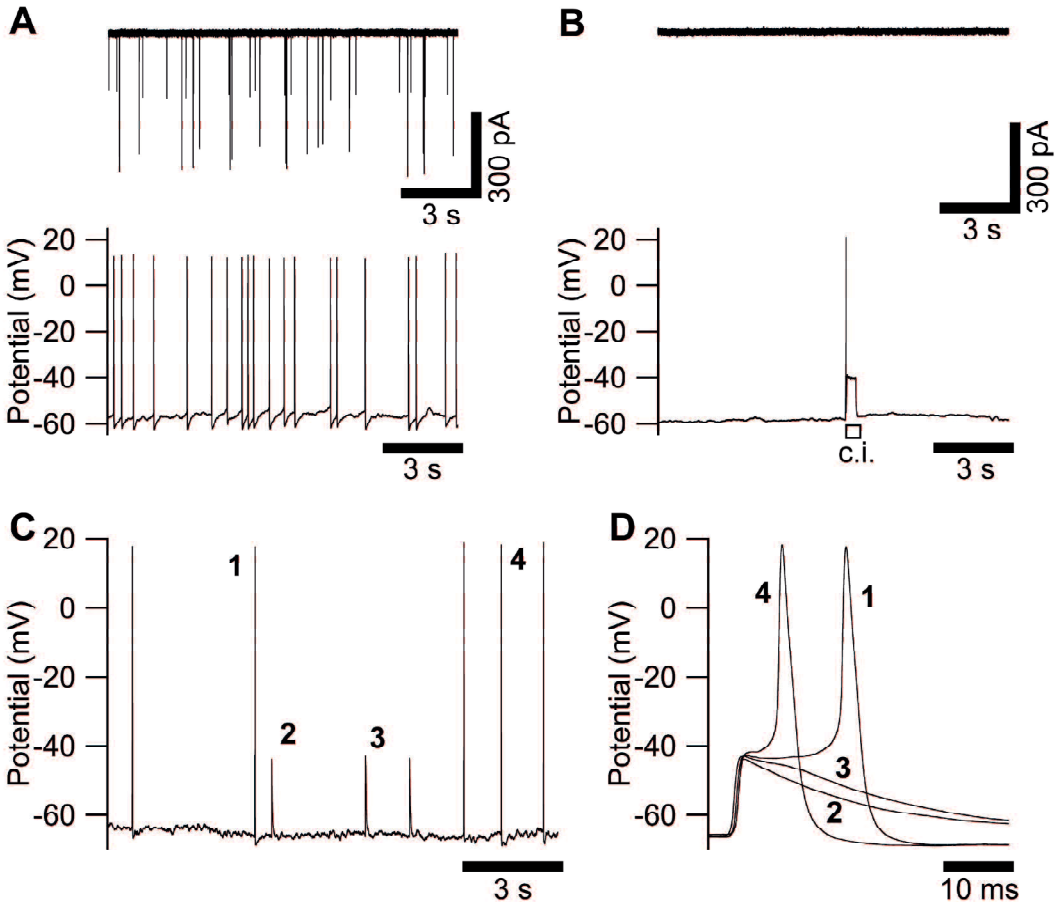

Fig. 10. Spontaneous action potentials were recorded from I_{sp}-generating neurons in the current clamp mode. (A, B) Voltage clamp recording at –50 mV (upper traces) and current clamp recording (lower traces) are shown in neurons generating I_{sp} (A) and no I_{sp} (B). A depolarizing command current was injected into neurons in B (c.i.) to evoke an action potential. (C) Another typical trace of current clamp recording in I_{sp}-generating neurons. (D) Time expanded traces numbered 1-4 in C are superimposed.

spontaneous discharge in the small compartments that were loosely voltage- or current-clamped in the whole-cell configuration. It is likely that, complete APs with overshoots may be generated when such small spikes induced depolarization of the whole-somatic membrane overcoming a threshold level for the AP. In addition, similarly to the effects on I_{sp}, TTX (100 nM), lidocaine (1 mM) and the reduction of the extracellular Na^+ concentration to 100 mM resulted in reversible abolition of the spontaneous discharges under the current-clamped condition (data not shown).

Involvement of TRPV1 in generation of spontaneous action potentials

Ozaki et al. reported that NGF-induced $[Ca^{2+}]_i$ fluctuations were observed in capsaicin-sensitive neurons more frequently than in capsaicin-non-responsive neurons (Ozaki et al., 2009). In addition, all neurons that showed APs in the on-cell mode responded to capsaicin at 1 μM in voltage clamp recordings (15/15, data not shown). These results suggest that TRPV1 is involved in generations of spontaneous APs. We next investigated effects of capsazepine and N-(4-tert-butylphenyl)-4-(3-chloropyridin-2-yl)piperazine-1-carboxamide (BCTC), specific TRPV1 antagonists, on spontaneous APs. In our unpublished observations, we have confirmed that both capsazepine at 10μM and BCTC at 1μM abolished current

responses to capsaicin at 1 μM of voltage-clamped DRG neurons in our preparation (data not shown). After observing generations of spontaneous APs in cell-attached configurations, we applied capsazepine at 10 μM and BCTC at 1 μM for 2 min. An application of capsazepine reversibly abolished spontaneous APs (Fig. 11A). Similarly to the effect of capsazepine, the spontaneous APs were blocked by BCTC (Fig. 11B). Moreover, capsazepine and BCTC hyperpolarized the resting membrane potentials in the on-cell mode (Fig. 12).

Since TRPV1 could be involved in the generations of spontaneous APs, we tried to investigate the profile of the subpopulations of DRG neurons that become hyperexcitable due to NGF in the results section II. We measured $[Ca^{2+}]_i$ by Ca^{2+}-imaging technique. One of the advantages of this method is that it readily permits simultaneous recordings from many individual neurons.

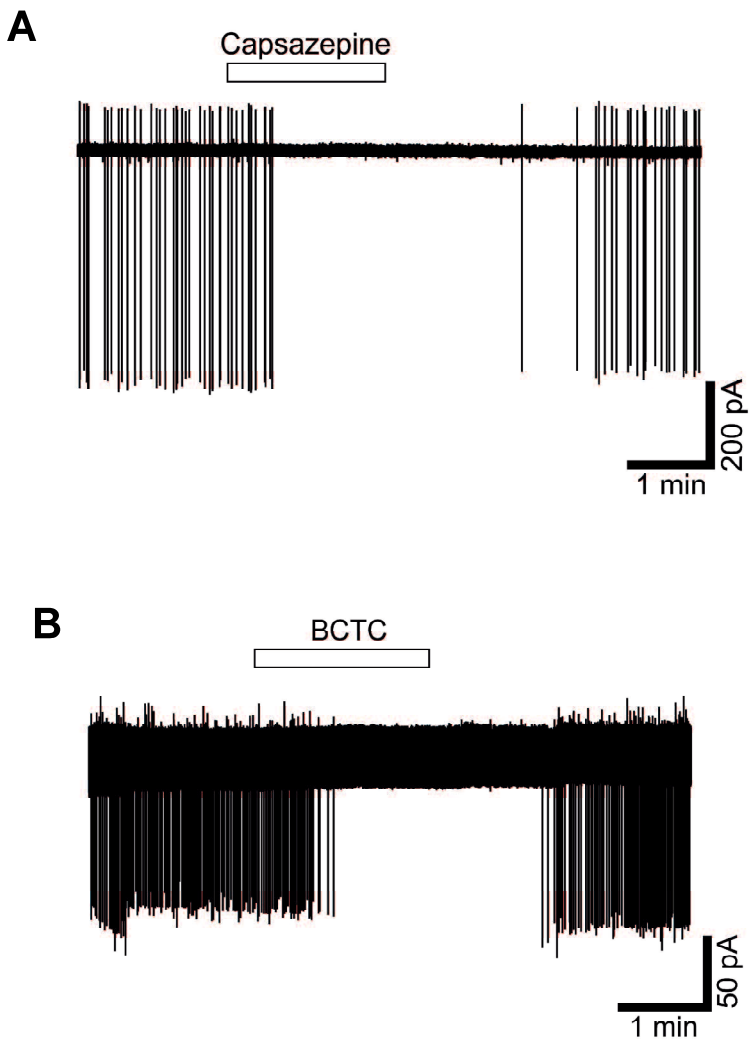

Fig. 11. Effects of TRPV1 antagonists, capsazepine and BCTC, on spontaneous APs in NGF-treated DRG neurons. Typical traces were shown. Capsazepine at 10 μM (A) and BCTC at 1 μM (B) were applied for 2 min to DRG neurons show spontaneous APs in on-cell mode.

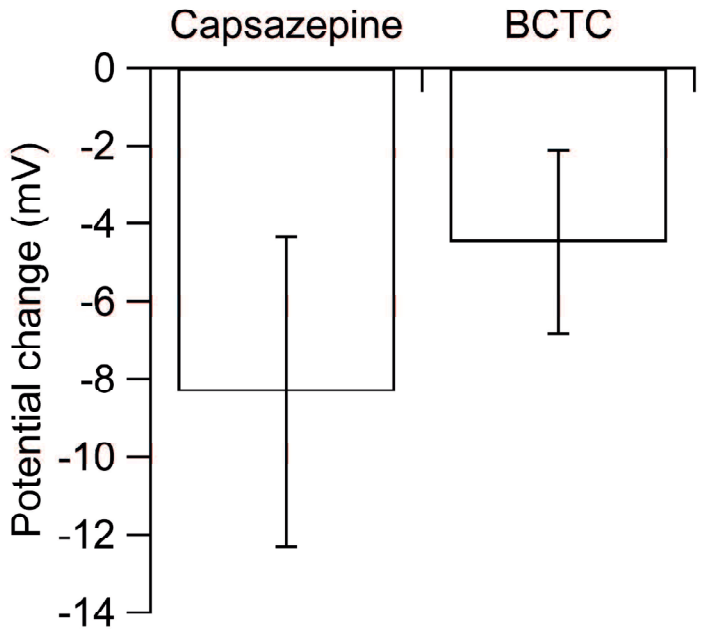

Fig. 12. TRPV1 antagonists induced membrane depolarization. The columns indicate the average values of membrane potential changes induced by an application of TRPV1 antagonists, capsazepine at 10 μM or BCTC at 1 μM for 2 min were compared with membrane potential before application of antagonist. Columns and vertical bars indicate the mean ± SEM.

RESULTS : II

$[Ca^{2+}]_i$ responses to capsaicin and icilin, and spontaneous fluctuations of $[Ca^{2+}]_i$

After the cells were cultured for more than 2 days in the presence or the absence of NGF, $[Ca^{2+}]_i$ was measured in Fura-2-loaded cells. When the cells were perfused with a solution containing 60 mM K^+ (60 K^+) for 30 s, $[Ca^{2+}]_i$ increased rapidly and transiently in some cells in both culture groups. Typical $[Ca^{2+}]_i$ responses to 60 K^+ in control cells cultured in the absence of NGF are shown in Fig. 13A. Under our experimental conditions, cells showing a $[Ca^{2+}]_i$ increase of more than 100 nM in response to a 30-s application of 60 K^+ were considered to be physiologically functional neurons. Capsaicin, perfused at 1 μM for 30 s, also caused rapid and transient $[Ca^{2+}]_i$ increases in subpopulations of the neurons in both the NGF-untreated and NGF-treated (the traces in Fig. 13B and C) groups. Icilin at 10 μM also caused rapid and transient $[Ca^{2+}]_i$ increases in subpopulations of the neurons in both NGF-untreated (Fig. 13C) and NGF-treated groups (Fig. 14; red and blue traces). A bright field image (Fig. 14B-a) and pseudocolor images of $[Ca^{2+}]_i$ of the cells in Fig. 14A before stimulation (b) and during stimulation by icilin (c) and capsaicin (d) are shown in Fig. 14B. The cell numbered 1 responded to capsaicin but not to icilin. The cells numbered 2 and 3 responded to both icilin and capsaicin. In the control neurons, the base lines of $[Ca^{2+}]_i$ were stable and silent as

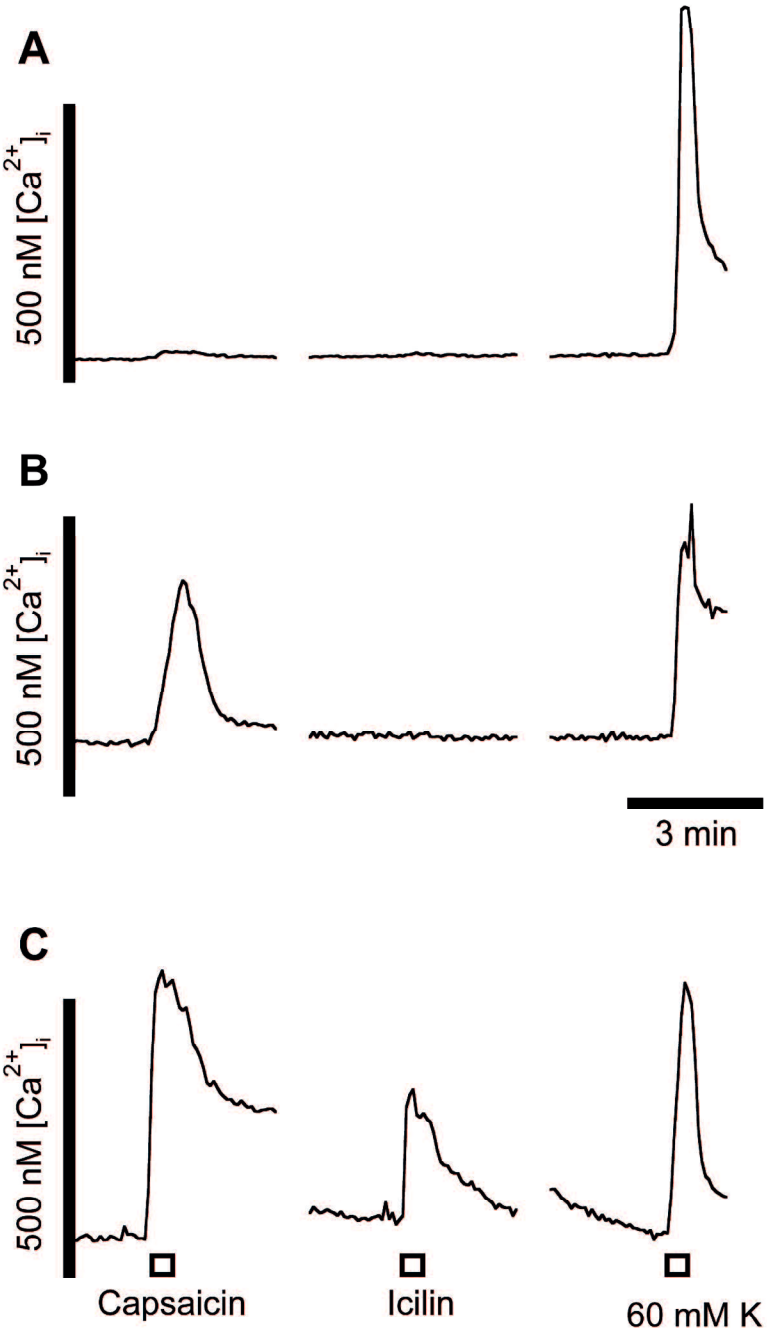

Fig. 13. $[Ca^{2+}]_i$ responses to capsaicin, icilin and high K^+ in cultured rat DRG neurons. Typical traces of $[Ca^{2+}]_i$ changes in 3 DRG neurons (A, B and C) cultured in the absence of NGF are shown. The traces in A, B and C were obtained simultaneously in the same recording field. Open bars indicate the application of capsaicin (1 μM), icilin (10 μM) and 60 mM K^+ for 30 s.

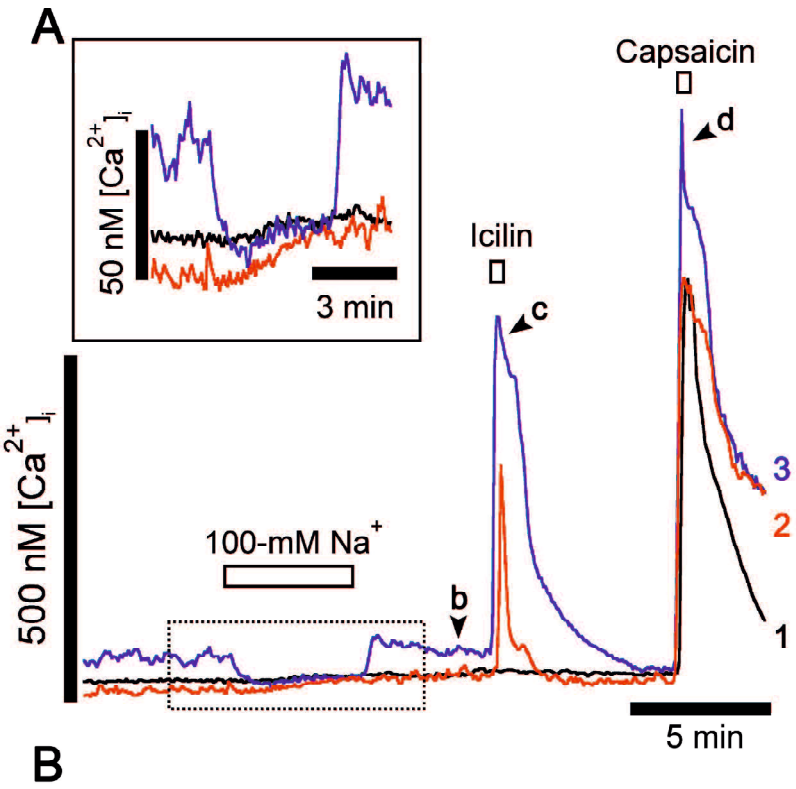
A
50 nM [Ca2+]i
3 min
Capsaicin
d
Icilin
c
500 nM [Ca2+]i
100-mM Na+
b
3
2
1
5 min
B
a
b
c
d
3
2
1
0
500 (nM)

Fig. 14. $[Ca^{2+}]_i$ responses to capsaicin, icilin in rat DRG neurons cultured in the presence of NGF (100 ng/ml). (A) Typical traces of $[Ca^{2+}]_i$ changes in 3 DRG neurons cultured in the presence of NGF are shown. A solution with a lower concentration of Na^+ (100 mM) was applied for 5 min as indicated by the open bars, followed by 30 s applications of icilin (10 μM) and capsaicin (1 μM) as indicated by the open bars. The inset in A shows expanded traces from the period indicated by the dotted-line box. (B) A bright field image (a) and pseudocolor images of $[Ca^{2+}]_i$ (b-d). Images b-d are before stimulation (b), during stimulation by icilin (c) and during stimulation by capsaicin (d). Cell numbers indicated in "d" correspond to the trace numbers in A. Scale bar = 100 μm.

shown in Fig. 12. In contrast, in some NGF-treated neurons, $[Ca^{2+}]_i$ spontaneously rose and fell as shown in the inset of Fig. 14A. These $[Ca^{2+}]_i$ fluctuations were reversibly reduced by decreasing the Na^+ concentration of the bath solution to 100 mM. This property is a fingerprint of $[Ca^{2+}]_i$ fluctuations in NGF-treated DRG neurons (Ozaki et al., 2009). To examine where intracellular Ca^{2+} came from during the fluctuation, an effect of reduction of Ca^{2+} in the extracellular solution was observed (Fig. 15A). When cells were perfused with the Ca^{2+}-free solution, the level of $[Ca^{2+}]_i$ and the amplitude of spontaneous $[Ca^{2+}]_i$ rise and fall were reduced. The degree of spontaneous $[Ca^{2+}]_i$ fluctuations was quantitatively assessed according to an analytical procedure reported previously (Ozaki et al., 2009). To obtain baseline levels of $[Ca^{2+}]_i$ in which spontaneous fluctuations were excluded, moving averages of $[Ca^{2+}]_i$ were calculated for 20 s at each time point, i.e. the moving averages of $[Ca^{2+}]_i$ were calculated from 5 values consisting of the values at each time point (Fig. 15B). On the assumption that this 20-s moving average of $[Ca^{2+}]_i$ indicated the baseline level, differences between the baseline levels and the actual $[Ca^{2+}]_i$ recorded were calculated (Fig. 15C). The differences between these two values were taken as the index indicating the fluctuations of $[Ca^{2+}]_i$ at relatively high frequency, which excluded spontaneous and slow changes in $[Ca^{2+}]_i$. In this study, these differences between the actual $[Ca^{2+}]_i$ and the moving

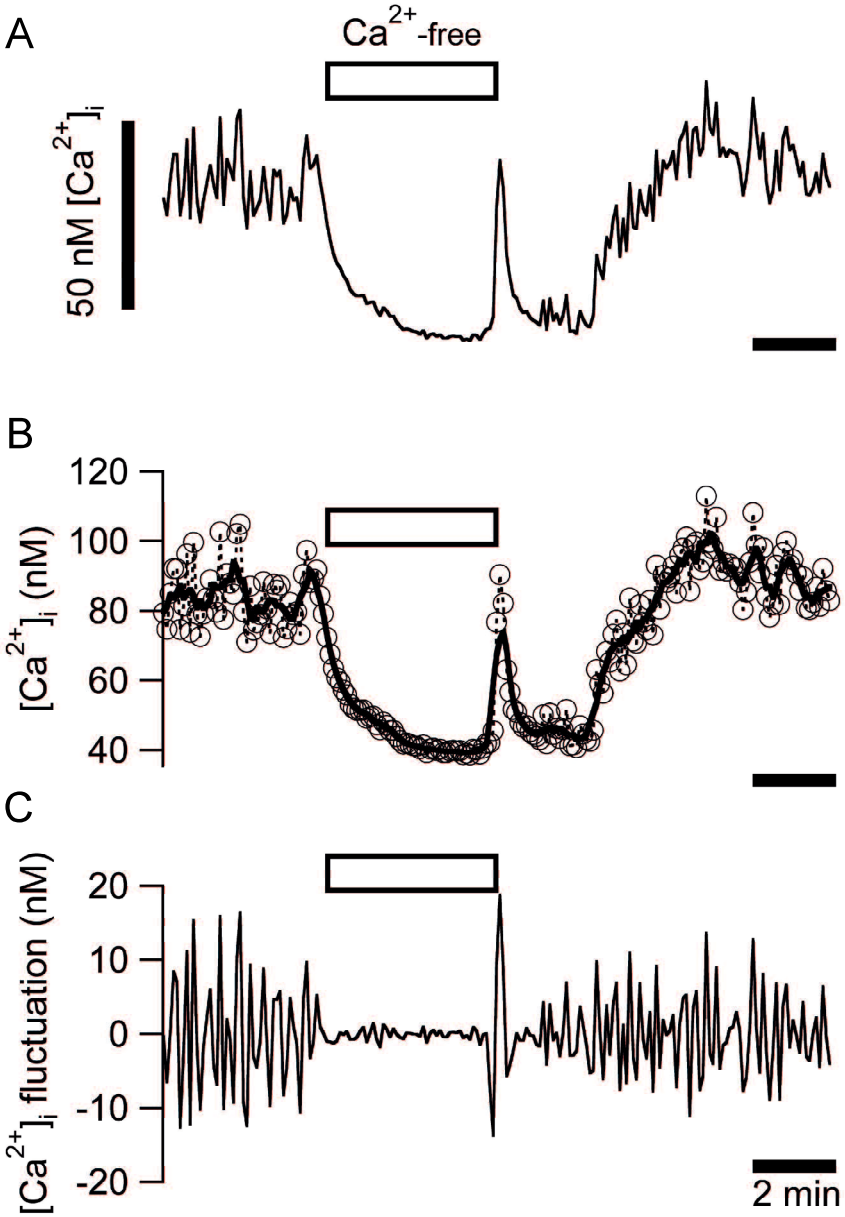

Fig. 15. Effects of Ca^{2+} removal on $[Ca^{2+}]_i$ fluctuation in rat DRG neurons cultured in the presence of NGF (100 ng/ml). (A) Typical traces of $[Ca^{2+}]_i$ changes in a DRG neuron cultured in the presence of NGF are shown. A solution without Ca^{2+} was applied for 5 min as indicated by the bar. (B) The same $[Ca^{2+}]_i$ response is shown. Actual $[Ca^{2+}]_i$ changes (open circles and adotted line) and calculated moving average for 20 s (a solid line) are plotted. (C) Differences between the actual $[Ca^{2+}]_i$ and the 20-s moving average (open circles minus solid line in B) are plotted. This difference is defined as "the $[Ca^{2+}]_i$ fluctuation" excluding slow and spontaneous change in $[Ca^{2+}]_i$ in this study.

averages are defined as "the $[Ca^{2+}]_i$ fluctuations". The variability of the $[Ca^{2+}]_i$ fluctuations was quantitatively expressed by the SD of the $[Ca^{2+}]_i$ fluctuations (nM). Moreover, effects of VGCC blockers and an inhibitor of Ca^{2+}-ATPase of the intracellular Ca^{2+} store were examined. Summarized data are shown in Fig. 16. The Ca^{2+}-free solution, the solution containing of nifedipine (1 μM), SNX-482 (0.2 μM), ω-agatoxin IVA (0.1 μM) and ω-conotoxin GVIA (1 μM), and the solution containing CPA (10 μM) were applied for 5 min. In NGF-treated neurons whose SD of the $[Ca^{2+}]_i$ fluctuation was significantly decreased by the reduction of extracellular Na^+ concentration, the SD of the $[Ca^{2+}]_i$ fluctuation significantly decreased by the reduction of Ca^{2+} and the VGCC blockers, but not by CPA (Fig. 16).

The relationship between the responsiveness to capsaicin and icilin

To clarify the profiles of different subgroups of DRG neurons, the correlation between the amplitudes of the $[Ca^{2+}]_i$ responses to capsaicin and icilin was analyzed in individual neurons. The amplitudes of the $[Ca^{2+}]_i$ responses to icilin are plotted against those to capsaicin in neurons of the control and NGF-treated groups (Fig. 17). In the present experiment, $[Ca^{2+}]_i$ rises of more than 50 nM (dotted lines in both plots) were considered as positive responses. In 69 control neurons tested, 35 neurons responded to

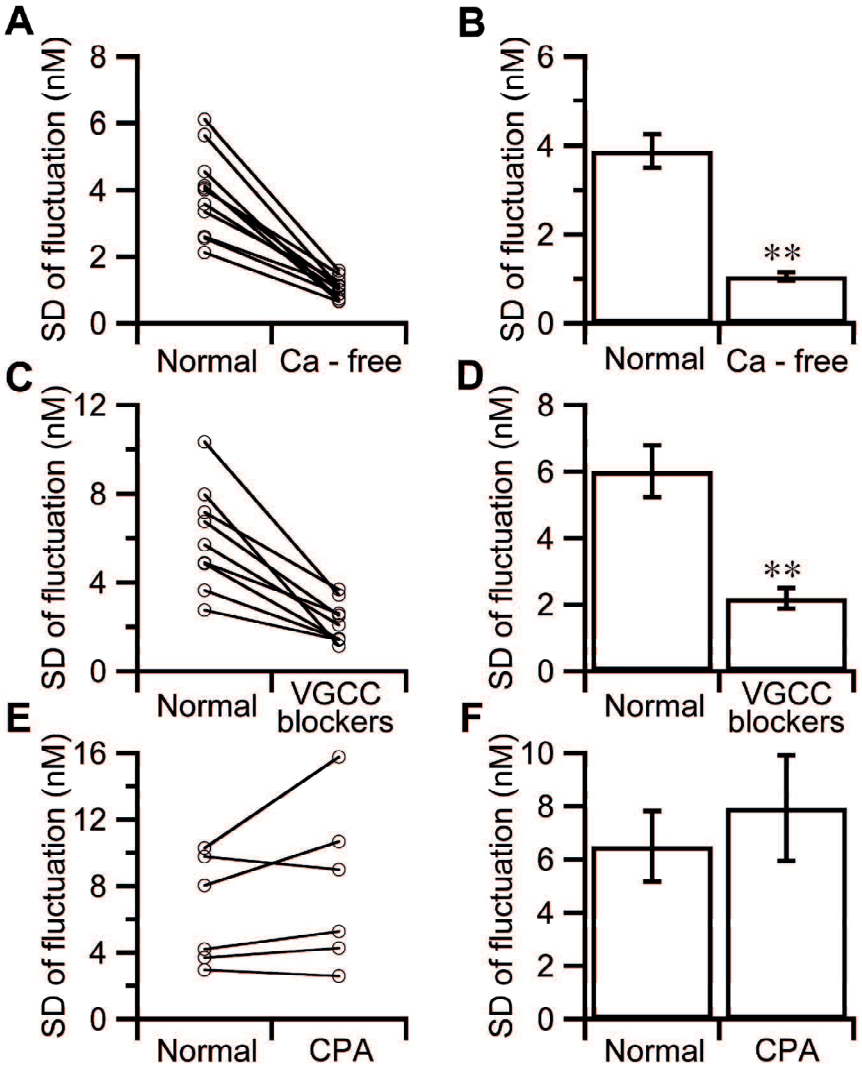

Fig. 16. Effect of Ca^{2+} removal, VGCC blockers and an inhibitor of Ca^{2+}-ATPase of the intracellular Ca^{2+} store on SD of the $[Ca^{2+}]_i$ fluctuation. (A, C, E) SD values of the $[Ca^{2+}]_i$ fluctuation before and during removing extracellular Ca^{2+} (A), applying VGCC blocker cocktail (nifedipine, SNX-482, ω-conotoxin GVIA and ω-agatoxin IVA) (C) and CPA (E) in 11, 9 and 6 NGF-treated neurons are plotted. The neurons were exposed to each solution for 5 min. The SD of the $[Ca^{2+}]_i$ fluctuation were calculated from data for 3 min just before, data for 3 min from 2 min after the beginning of the application of each solution. (B, D, F) Summarized data of the SD of the $[Ca^{2+}]_i$ fluctuation. The columns indicate the average of the SD of the $[Ca^{2+}]_i$ fluctuation in the normal solution and in the Ca^{2+}-free solution (B), in the presence of VGCC blockers (D) and CPA (F). Columns and vertical bars indicate the mean ± SEM. $^{**}p < 0.01$ by paired *T*-test.

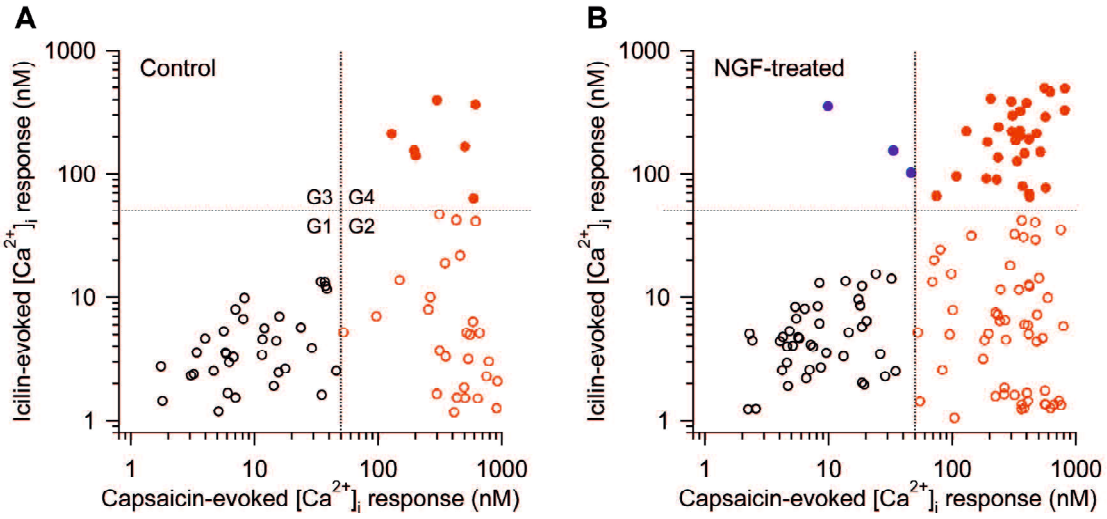

Fig. 17. The relationship between $[Ca^{2+}]_i$ responses to capsaicin and icilin in control (A) and NGF-treated (B) DRG neurons. The amplitudes of the icilin-evoked $[Ca^{2+}]_i$ responses are plotted against those of the capsaicin-evoked $[Ca^{2+}]_i$ responses in the identical DRG neurons. Dotted lines indicate the level of $[Ca^{2+}]_i$ responses of 50 nM. Neurons are divided into 4 groups as indicated in A (G1-G4). Neurons in different groups are shown by different symbols.

capsaicin (about 50%). Among these capsaicin-responsive neurons, only 7 neurons responded to icilin as well. On the other hand, no icilin-responsive neuron was found among the 34 neurons that did not respond to capsaicin. According to their responsiveness to capsaicin and icilin, DRG neurons were divided into 4 groups: subpopulations of neurons not responding to either capsaicin or icilin (group 1; G1, open circles in Fig. 17), neurons responding to capsaicin but not to icilin (group 2; G2, red open circles in Fig. 17), neurons responding to icilin but not to capsaicin (group 3; G3, blue solid circles in Fig. 17) and neurons responding to both capsaicin and icilin (group 4; G4, red solid circles in Fig. 17). From a total of 131 NGF-treated neurons, 87 neurons responded to capsaicin (groups 2 and 4). Among these, 32 neurons also responded to icilin (group 4). On the other hand, among 44 neurons that did not respond to capsaicin (groups 1 and 3), only 3 neurons responded to icilin (group 3).

$[Ca^{2+}]_i$ fluctuations in subgroups of DRG neurons

To clarify whether there is a correlation between the capsaicin and icilin responsiveness of DRG neurons and the induction of $[Ca^{2+}]_i$ fluctuations by chronic NGF treatment, the SD of the $[Ca^{2+}]_i$ fluctuations was plotted against the amplitudes of the $[Ca^{2+}]_i$ responses to capsaicin and icilin (Fig. 18). In control neurons cultured in the

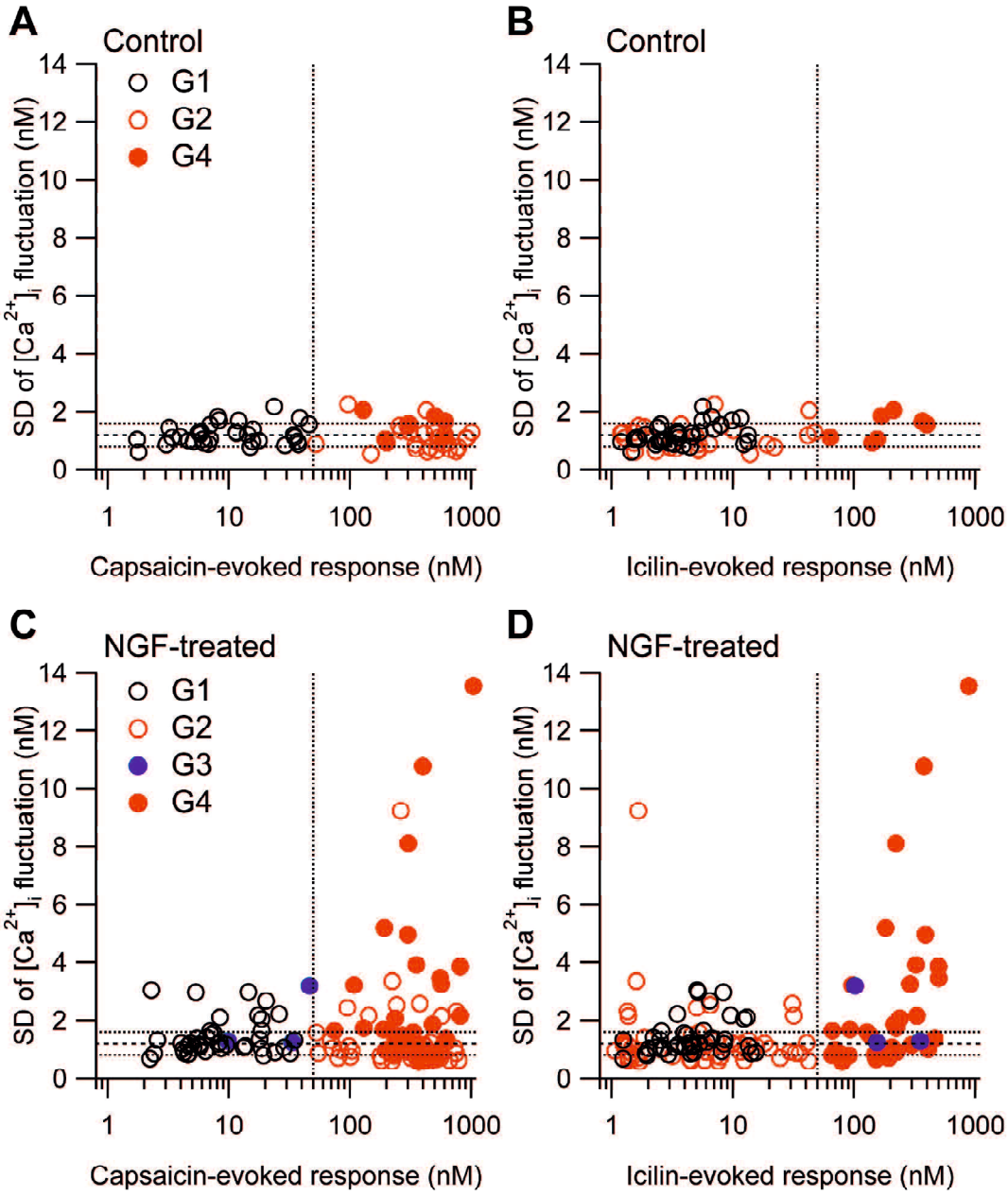

Fig. 18. The relationship between the variability of $[Ca^{2+}]_i$ fluctuations and the amplitudes of capsaicin- and icilin-evoked $[Ca^{2+}]_i$ responses in control (A and B) and NGF-treated (C and D) DRG neurons. The SD of the $[Ca^{2+}]_i$ fluctuations is plotted against the amplitudes of the $[Ca^{2+}]_i$ responses to capsaicin (A and C) and icilin (B and D) of the identical neurons. Neurons in the different groups defined in Fig. 3 are shown by different symbols, identical to those in Fig. 3. The horizontal dotted lines indicate the mean ± SDM of the SD of the $[Ca^{2+}]_i$ fluctuations in control neurons (1.2 ± 0.4 nM), and the vertical dotted lines indicate the level of $[Ca^{2+}]_i$ responses of 50 nM.

absence of NGF, no clear $[Ca^{2+}]_i$ fluctuations were observed (left 2 plots in Fig. 18). The average and the SDM value of the SD of the $[Ca^{2+}]_i$ fluctuations of the control neurons were 1.20 ± 0.39 nM (n = 69, horizontal dotted lines in Fig. 18). In contrast, in NGF-treated neurons, 29 out of 131 neurons showed larger $[Ca^{2+}]_i$ fluctuations whose SD was more than 2 nM. Moreover, in these 29 neurons showing such large $[Ca^{2+}]_i$ fluctuations, 8, 8, 1 and 12 neurons were in groups 1, 2, 3 and 4, respectively. Six neurons showed large fluctuations of $[Ca^{2+}]_i$ (SD > 4 nM). Among these 6 neurons, 5 neurons were in group 4 and only 1 neuron was in group 2.

To quantitatively assess the $[Ca^{2+}]_i$ fluctuations in the subgroups of DRG neurons, the mean and the SEM of the SD of the $[Ca^{2+}]_i$ fluctuations in each subgroup was calculated, and ANOVA was used for statistical analysis (Fig. 19). In the control neurons cultured in the absence of NGF, no significant difference was detected among 3 subgroups ($p > 0.05$, $F = 2.27$). In contrast, in the neurons cultured in the presence of NGF, significant differences were detected among 4 subgroups ($p < 0.01$, $F = 5.06$), between group 1 and group 4 ($p < 0.01$, $F = 7.53$), and between group 2 and group 4 ($p < 0.01$, $F = 9.44$). Statistical significance between group 3 and the other subgroups could not be assessed because of the small number of neurons found in group 3. Between the control and NGF-treated neurons, a statistically significant difference in

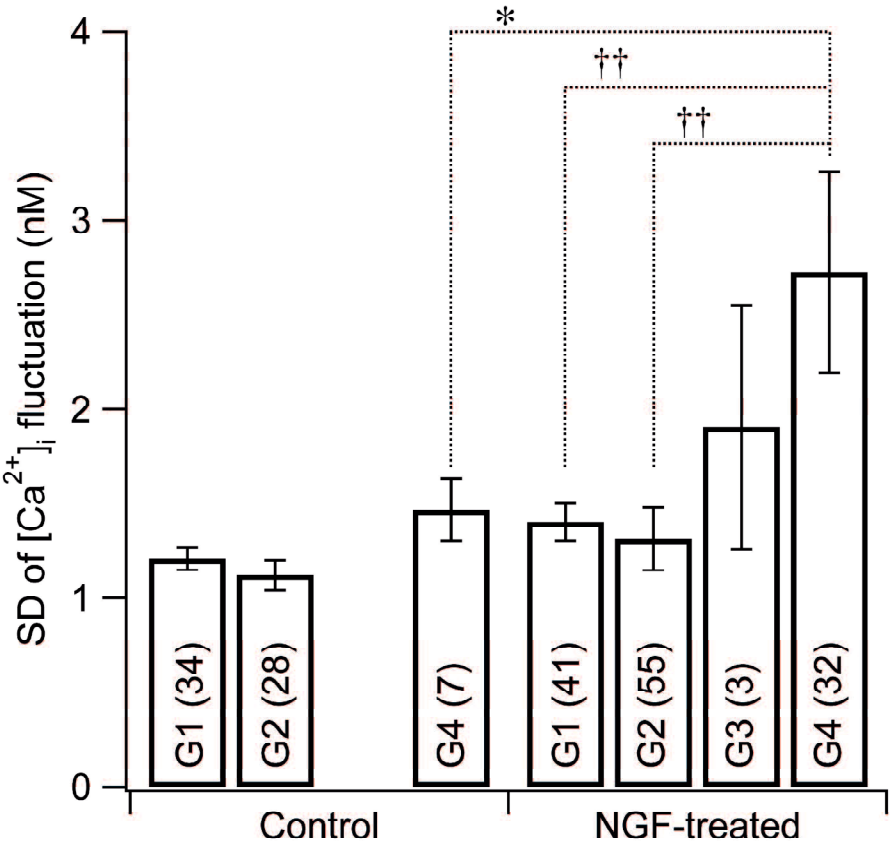

Fig. 19. The variability of $[Ca^{2+}]_i$ fluctuations in different groups of control and NGF-treated neurons. The averages of the SD of the $[Ca^{2+}]_i$ fluctuations in Groups 1 (G1) to 4 (G4) of control and NGF-treated neurons are shown by columns. The numbers in parentheses indicate the numbers of neurons in each group. * $p < 0.05$ by *T*-test, †† $p < 0.01$ by ANOVA.

the SD of the $[Ca^{2+}]_i$ fluctuations was detected only in group 4 neurons ($p < 0.05$ by *T*-test).

DISCUSSION

Spontaneous action potentials and Ca^{2+} source of $[Ca^{2+}]_i$ fluctuations

I confirmed that the chronic treatment of DRG with NGF induces the spontaneous APs and the $[Ca^{2+}]_i$ fluctuations in subpopulations of cultured DRG neurons in accordance with previous reports (Kitamura et al., 2005; Ozaki et al., 2009). Since the $[Ca^{2+}]_i$ fluctuations are inhibited by a decrease in the concentration of extracellular Na^+, TTX and lidocaine, they are likely to result from spontaneous APs (Ozaki et al., 2009). Intracellular Ca^{2+} has important roles not only in transmitter release, but also in gene expression, regulation of membrane excitability and survival of neurons. I determined the Ca^{2+} source contributing to the spontaneous fluctuations of $[Ca^{2+}]_i$. The Ca^{2+} removal from the extracellular solution and the VGCC blockers reduced the SD of the $[Ca^{2+}]_i$ fluctuations. On the other hand, CPA did not affect $[Ca^{2+}]_i$ fluctuations. It appears that repetitive activation of VGCC by the repetitive action potentials but not Ca^{2+} mobilization from the intracellular Ca^{2+} store are the underlying mechanism of the $[Ca^{2+}]_i$ fluctuations. In the next series of experiments, I tried to investigate the mechanisms of the generation of spontaneous APs.

The mechanisms of spontaneous action potentials generation in NGF-treated neurons

Among the DRG neurons cultured in the presence of NGF and generating spontaneous APs in the cell-attached configuration, 75% neurons showed I_{sp} under the whole-cell dialyzed and voltage-clamped conditions. In contrast, I_{sp} was recorded from only 4.3% of neurons showing no spontaneous firing in the on-cell mode. Therefore, I_{sp} is likely to relate closely to the spontaneous APs in intact neurons. Each I_{sp} had an initial inward phase and a subsequent outward phase that was inhibited by the K^+ channel blocking agents. The former could have resulted from the depolarizing phase of the discharge and the latter, the repolarizing phase. Namely, all results obtained in the whole-cell configuration supported our hypothesis that I_{sp} reflects the discharge occurring in a loosely voltage-clamped membrane region. Multiple kinds of I_{sp} with different amplitudes were recorded from the single DRG neuron (Fig. 4 to 8). The different kinds of I_{sp} in each neuron never interfered in their amplitudes and occurred independently, indicating that more than two compartments generating I_{sp} existed in single neuron. The difference in the membrane area of these compartments, i.e. the number of expressing ion channels related with the discharge, may result in the difference in the amplitude of I_{sp}. Taking into consideration that I_{sp} was recorded under the voltage-clamped condition, I_{sp} was physically an error of the voltage clamping. However, since this phenomenon was induced by the biological treatment, the chronic

treatment of DRG neurons with exogenous NGF, the induction of I_{sp} by NGF had biological significance.

Generally, DRG neurons extend dendrites and axons during culture. It is more difficult to clamp potentials of local membranes on the dendrite and axon than those on the soma in the whole-cell configurations, and spontaneous discharges were more likely to occur at membranes far from the soma. Amir et al. reported that somatic discharges of DRG neurons excised from nerve-injured rats were triggered by multiple ectopic sources and concluded that neuropathic DRG neurons had at least three sources to trigger the spontaneous firing (Amir et al., 2005). One was neuroma near the injured site and others were a subthreshold membrane potential oscillation (SMPO) of the soma and an ectopic discharge at T-junction. The activity of the last two sources was reported to depend on somatic membrane potential. In the NGF-treated hyperexcitable DRG neurons in this study, the SMPO was not evident in the current clamp mode. Since, even under the voltage-clamped condition, spontaneous activities recorded as I_{sp} were maintained, I_{sp} at high frequency might mask or compete the possible SMPO. In general, the outside-out patch configuration establishes a better voltage-clamped condition than the whole-cell configuration. While, surprisingly, I_{sp} was recorded from the excised outside-out patch membranes. The pharmacological and ionic properties and the

kinetics of I_{sp} in the excised patch membranes well resembled those in the whole-cell configuration, indicating that the loosely voltage-clamped compartment that discharged spontaneously existed within an excised patch-membrane. Since the tip of the recording pipettes holding the excised outside-out patch membranes was kept further than 5 mm from the soma, it was unlikely that the excised membranes were connected to the soma through a thin tube of the cytoplasmic membrane and the spontaneous discharges that occurred at the soma were recorded as an action current. Moreover, since the tips of the patch pipettes were placed on the center of the soma during the whole-cell recording, the excised patch membranes were derived from the somatic membrane. Although it was unclear what structures were included in the excised patch membranes and discharging spontaneously, it became evident that the triggering source of the whole-somatic action potential was included with in the soma itself of the DRG neurons.

Under the current-clamped conditions, in many NGF-treated hyperexcitable neurons, spontaneous APs with queer shapes were observed. Since, in these neurons, spontaneous discharges are expected to occur at multiple separated compartments on the somatic membrane, these activities are likely to be recorded as small depolarization under the current-clamped conditions. In the case when these small depolarizing spikes

overcame the threshold of the AP generation, complete APs with overshoots may be recorded after the small spikes. It was expected that sub-superficial environments below the loosely voltage-clamped compartments showing I_{sp} were not dialyzed well with the pipette solutions and remained intact relatively. Therefore, spontaneous discharges in small somatic regions causing I_{sp} probably played a role to trigger the whole-somatic APs in the NGF-treated DRG neurons.

DRG neurons isolated from neuropathic model rats are reported to have hypersensitivity to inflammatory mediators including bradykinin, serotonin, prostaglandin E_2 and histamine (Song et al., 2003). It is also reported that NGF acutely applied to the DRG neurons isolated from normal animals potentiates the sensitivity of TRPV1 to capsaicin (Shu and Mendell, 1999a; Shu and Mendell, 1999b; Shu and Mendell, 2001). These results suggest that nerve injury or NGF treatment cause the potentiation of activity of excitatory receptors in DRG neurons. However, such mechanisms may not contribute in the DRG neurons cultured in the presence of NGF in this study. Since we made the patch clamp recording in the neurons continuously perfused with the artificial physiological solutions, it is unlikely that an excitatory mediator, e.g. ATP or glutamate, released from surrounding cells acted on the recording neurons. Moreover, I_{sp} in the outside-out patch membranes excluded the possibility that

continuous or spontaneous excitatory synaptic inputs induced the spontaneous discharges at the loosely voltage-clamped local membranes far from the soma. Therefore, we concluded that the chronic treatment of DRG neurons with NGF provided some intrinsic cellular mechanism causing the abnormal hyperexcitability to discharge spontaneously.

The upregulation of excitatory ion channels on the soma could be a possible underlying mechanism. It was reported that NGF regulated the expression of the voltage-gated Na^+ channel: the NGF receptor, trk A, correlated with one of the voltage-gated Na^+ channel, $Na_V1.8$, in the sensory neurons (Fang et al., 2005), and NGF incereased the expression level of TTX-resistant Na^+ channles in DRG neurons (Fjell et al., 1999). To clarify whether the upregulation of TTX-resistant Na^+ channels contributes to the spontaneous firing, we examined correlation between frequencies of spontaneous firing in the on-cell mode and current densities of Na^+ current through TTX-sensitive and TTX-resistant Na^+ channels. Significant correlation was not detected (data not shown), indicating that the expression levels of certain subtypes of the voltage-gated Na^+ channel are not the critical factor to cause the spontaneous firing in the NGF-treated rat DRG neurons.

I next examined what causes the activation of voltage-gated Na^+ channels. The

spontaneous APs were reversibly inhibited by the selective TRPV1 antagonists. An application of these antagonists also induced hyperpolarization. It was reported that chronic treatment of DRG neurons with NGF regulated the expression and activity of TRPV1 (Winter et al., 1988; Ji et al., 2002; Galoyan et al., 2003; Price et al., 2005; Anand et al., 2006). I examined the correlation between the density of capsaicin-induced currents and the frequencies of spontaneous APs. Positive correlations were not detected (data not shown). These results suggest that the changes in the TRPV1 channel activity, but not the change in TRPV1 expression levels, cause membrane depolarization in DRG neurons treated with NGF. Moreover, this changes in the TRPV1 activity occurs without any ligand that activates TRPV1. Since removal of extracellular Ca^{2+} did not affect the generation of spontaneous APs (Fig. 6D), the main charge carrier of TRPV1 may be Na^{+}. Considering the results that the resting membrane potentials between I_{sp}-generating neurons and neurons that showed no I_{sp} were not different, Na^{+} influx through the activated TRPV1 in the small fractions of the membrane may activate VGSC and generate APs.

Most icilin-responding neurons respond to capsaicin

The spontaneous APs or $[Ca^{2+}]_i$ fluctuations were recorded in subpopulation of

DRG neurons cultured in the presence of NGF. It has been reported that NGF-induced $[Ca^{2+}]_i$ fluctuations were observed in small and medium size neurons and in capsaicin-sensitive neurons more frequently than in capsaicin-non-responsive neurons (Ozaki et al., 2009). In order to further distinguish the profiles of the DRG neurons that became hyperexcitable due to NGF, $[Ca^{2+}]_i$ responses to capsaicin and icilin were examined by Ca^{2+} -imaging technique. In DRG neurons, capsaicin has been reported to induce a $[Ca^{2+}]_i$ rise by stimulating Ca^{2+} influx through TRPV1 channels and Ca^{2+} efflux from the intracellular Ca^{2+} store (Eun et al., 2001; Liu et al., 2003; Kárai et al., 2004; Hagenacker et al., 2008), icilin has been reported to induce a $[Ca^{2+}]_i$ rise by evoking Ca^{2+} influx through TRPM8 and TRPA1, which are also Ca^{2+} permeable channels (Story et al., 2003; Andersson et al., 2004; Babes et al., 2004). In the present study, both capsaicin and icilin induced a transient rise in $[Ca^{2+}]_i$ in the subpopulations of neurons, regardless of the treatment with NGF. Since the $[Ca^{2+}]_i$ responses to icilin rose and fell more rapidly than those to capsaicin, we applied icilin before capsaicin application. In control neurons, about half of the neurons responded to capsaicin and about 10% responded to icilin. It was reported that TRPV1 and TRPA1 were cross-desensitized each other (Akopian et al., 2008; Ruparel et al., 2008; Akopian et al., 2009). Therefore, the responsiveness to capsaicin estimated by the $[Ca^{2+}]_i$ responses in

this study might be underestimated. Even though, in our preparations, almost of all icilin-responding neurons also responded to capsaicin, suggesting that icilin-sensitive TRPs are always expressed together with TRPV1. It was reported that TRPV1 and TRPM8 were not coexpressed, and that TRPA1 was always expressed together with TRPV1 in rat DRG neurons, based on the results of *in situ* hybridization experiments (Story et al., 2003; Kobayashi et al., 2005). Taken together, these findings suggest that icilin may act on TRPA1-expressing neurons (group 4) to evoke a rise in $[Ca^{2+}]_i$. This was also the case in NGF-treated neurons: among 35 icilin-responding neurons, 32 neurons responded to capsaicin. It was reported that NGF-treatment affects the expression level and pattern of TRPM8 in cultured DRG neurons (Story et al., 2003; Babes et al., 2004; Luo et al., 2007). Therefore, it is possible that in our experiments, NGF up-regulated TRPM8 (and/or TRPA1) and caused the appearance of neurons responding to icilin but not to capsaicin in the NGF-treated group, although the number of such neurons was very meager (3 out of 131).

$[Ca^{2+}]_i$ fluctuations were observed in icilin-responding neurons

Ozaki et al. reported that the proportion of neurons with the variable $[Ca^{2+}]_i$ fluctuations (SD > 2 nM) is small in the capsaicin-non-responsive neurons in

comparison with capsaicin-sensitive-neurons (Ozaki et al., 2009). In my configuration, fluctuations of $[Ca^{2+}]_i$ whose SD was more variable than 2.5 nM were never observed in control neurons. In the subpopulation of NGF-treated neurons, large spontaneous fluctuations of $[Ca^{2+}]_i$ were observed. In 19 of 131 NGF-treated neurons, the SD of the $[Ca^{2+}]_i$ fluctuations was more variable than 2.5 nM, indicating that chronic treatment of DRG neurons with NGF induces the chronic appearance of potentiated $[Ca^{2+}]_i$ fluctuations. In the NGF-treated neurons of group 1 that responded neither to capsaicin nor to icilin, there were 4 neurons out of 41 that showed $[Ca^{2+}]_i$ fluctuations with an SD more variable than 2.5 nM. In these neurons, the SD never exceeded 3.1 nM. In contrast, among capsaicin-responding neurons (group 2 and 4), 12 of 87 neurons showed $[Ca^{2+}]_i$ fluctuations with an SD exceeding 3 nM. Among these 12 neurons, 10 neurons were in group 4, indicating that icilin-responding neurons tended to show $[Ca^{2+}]_i$ fluctuations with larger amplitudes. These results concerning the SD of the $[Ca^{2+}]_i$ fluctuations are summarized in Fig. 19. It should be noted that there was no significant difference in the average of the SD of the $[Ca^{2+}]_i$ fluctuations between neurons in groups 1 and 2 of NGF-treated neurons. However, the SD of group 4 of the NGF-treated neurons was significantly more variable than that of groups 1 and 2. Ozaki et al. suggested that capsaicin-responding nociceptive neurons were affected by NGF more frequently and

became hyperexcitable (Ozaki et al., 2009). I conclude here that DRG neurons responding to both capsaicin and icilin are affected by NGF more effectively than neurons responding only to capsaicin, and that the former become hyperexcitable. As mentioned above, spontaneous APs were abolished by the TRPV1 antagonists. These results suggest that TRPV1 play a crucial role in generation of APs. However $[Ca^{2+}]_i$ fluctuations were observed also in capsaicin-non-responsive neurons. Therefore, it is possible that chronic treatment with NGF could affect TRPV1 activity without changing sensitivity to capsaicin.

Pathophysiological significance of hyperexcitable nociceptors in neuropathic pain

In our preparations, the diameter of the soma of the DRG neurons used in our laboratory ranged between 15 and 35 μm. Neurons in this range are generally classified as small to medium size neurons, including nociceptive Aδ- and C-neurons. One of the characteristics of nociceptive neurons is the expression of TRPV1. The present results show that the subpopulation of TRPV1-expressing neurons also expresses cold-sensing TRP, and that these neurons are made hyperexcitable by NGF. It was reported that TRPM8 is not coexpressed with TRPV1 and that TRPA1 is coexpressed with TRPV1 in rat DRG neurons (Story et al., 2003; Kobayashi et al., 2005). Therefore, it seems that

icilin acts on TRPA1- and TRPV1-expressing neurons and evokes the $[Ca^{2+}]_i$ rise. NGF generally acts on the two types of NGF receptors, TrkA and $p75^{NTR}$, in DRG neurons (Verge et al., 1989; Mu et al., 1993; Sebert and Shooter, 1993; Verge et al., 1995), and it was confirmed that both TrkA and $p75^{NTR}$ are expressed in cultured DRG neurons (Kitamura et al., 2005). It was reported that 70% of DRG neurons express TrkA at the neonatal stage, but that the population of TrkA-expressing neurons decreases with maturation, with about 40% of the cells expressing TrkA at 14 days after birth (Bennett et al., 1996). Further, TrkA is expressed in DRG neurons expressing TRPV1, TRPM8 and TRPA1 in the adult rat (Kobayashi et al., 2005). Taken together, it can be concluded that TrkA is coexpressed with TRPV1 and TRPA1 in cultured rat DRG neurons and that the activation of TrkA by NGF results in hyperexcitability. The dual reaction of DRG neurons to icilin and capsaicin suggests that such neurons do not act as simple cold-sensing or hot-sensing neurons, but rather that they act as non-specific nociceptive neurons. The physiological roles of TRPM8 and TRPA1 in cold-sensing are controversial. Many lines of evidence indicate that TRPM8 is activated by a moderate lowering of temperature and that a greater decrease in temperature is required for the activation of TRPA1. Although there is no doubt that cold stimulation activates sensory neurons expressing TRPM8/A1, it is not certain that such information is recognized as a

cold sensation by the CNS. It has been reported that TRPA1 has a pronociceptive role in the mouse (Andrade et al., 2008), suggesting that TRPA1-expressing sensory neurons could be nociceptive neurons. Therefore, it is expected that DRG neurons expressing both TRPV1 and TRPA1, probably group 4 neurons in this study, have physiological roles as nociceptors. It is likely that NGF acts on group 4 neurons and makes them hyperexcitable. Therefore, if this action of NGF on group 4 neurons occurs *in vivo*, it may cause a hyperalgesic sensation.

CONCLUSION

In this study, we demonstrated that NGF-treated DRG neurons show the spontaneous APs that could be induced by Na^+ influx through TRPV1 in the absence of any stimuli. Moreover, the amplitude of the $[Ca^{2+}]_i$ fluctuations was significantly larger in neurons sensitive to both capsaicin and icilin than that in the other neurons. Since these neurons are considered to be the nociceptor, it appears that NGF acts on the nociceptive DRG neurons and makes them hyperexcitable. If the intrinsic changes in the excitability of the somatic membranes of the nociceptive DRG neurons by NGF observed in this study occurred also *in vivo*, these hyperexcitable DRG neurons may cause unusual pains, such as hyperalgesia of allodynia. Molecular basis of the underlying mechanism of the hyperexcitability is not clear at present. Further investigation of properties of hyperexcitable neurons is needed to clarify the pathogenic mechanism of the neuropathic pain**.**

ACKNOWLEDGEMENTS

I would like to express my sincere gratitude to my supervisor, Dr. Izumi Shibuya, Professor, Department of Veterinary Medicine, Faculty of Agriculture, Tottori University, Japan, for providing me this precious study opportunity as a Ph.D student in his laboratory.

I especially would also like to express my deepest appreciation to my supervisor, Dr. Naoki Kitamura, Associate professor, Department of Veterinary Medicine, Faculty of Agriculture, Tottori University, Japan, for his elaborated guidance, considerable encouragement and invaluable discussion that make my research of great achievement and my study life unforgettable.

I sincerely wish to appreciate Dr. Govindan Dayanithi, Professor, Department of Cellular Neurophysiology, Institute of Experimental Medicine, Academy of Science of the Czech Republic, Dr. Emil Toescu, Associate Professor, Department of Physiology, School of Medicine, Birmingham University, UK, Dr. Yasuaki Kawasaki, Professor, Department of Behavioral Physiology and ecology, Joint Faculty of Veterinary Medicine, Kagoshima University, Japan, Dr. Toshio Ohta, Professor, Department of Veterinary Pharmacology, Faculty of Agriculture, Tottori University and Dr. Kenji Takahashi, Associate professor, Department of Veterinary Pharmacology, Faculty of

Agriculture, Tottori University, Japan, for their intimate advice and comments to my research projects and thesis.

I am very grateful also to Taiki Moriya, PhD student in our laboratory, Atsushi Tsutsumi, Hyogo prefecture, Yui Ozaki, Takeshi kuwahara, Kuwahara Animal Hospital (Osaka, Japan), You Komagiri, Lecturer, Department of Physiology, Faculty of Medicine, Iwate Medical University, Japan, and the students in this laboratory for their valuable cooperation in my experiments.

This study was supported by a research grant from KAKENHI (Grant #: 16780200, 18380175,25450463, 25450464), and Grant-in-Aid for JSPS Fellows. Dr. G.Dayanithi is supported by Japan Society for the Promotion of Science Invitation Fellowship Program (ID#FY2008; S-08216).

I would like to extend my indebtedness to my family for their endless love, understanding, support, encouragement and sacrifice throughout my study.

Finally, I would like to thank and pay my respects to animals for giving excellent data in my study.

SUMMARY

[INTRODUCTION & PURPOSE]

Peripheral nerve injury frequently results in severe chronic pain, neuropathic pain. Although the pathogenic mechanism of neuropathic pain is poorly understood, nerve growth factor (NGF) is considered to be one of candidate mediators of the pathogenesis. NGF promotes the survival of embryonic sensory neurons and maintains the phenotypic characteristics of primary nociceptive neurons postnatally. In adults, however, NGF also contributes to nociceptor activation and hyperalgesia after nerve injury and during inflammation. For example, it has been reported that intrathecal administration of NGF applied in adult rats resulted in hyperalgesia, and that the NGF concentration in the dorsal root ganglion (DRG) increased after an artificial nerve injury. It is also reported that adult rat DRG neurons cultured in the presence of NGF at 100 ng/ml generate spontaneous action potentials (APs) and show spontaneous fluctuations of the intracellular Ca^{2+} concentration ($[Ca^{2+}]_i$). However, the mechanism of the somatic hyperexcitablity to fire spontaneously in the NGF-treated DRG neurons remains unclear. To investigate underlying mechanisms triggering the spontaneous discharges in the NGF-treated DRG neurons in culture, voltage clamp and current clamp recordings in the whole-cell and outside-out configurations were made. Moreover, it is also unclear

what types of DRG neurons become hyperexcitable in response to NGF. In order to investigate the profile of the subpopulations of DRG neurons that become hyperexcitable by NGF treatment, patterns of changes in $[Ca^{2+}]_i$ were used as a index of cellular activity. In particular, I focused on $[Ca^{2+}]_i$ responses to the two ligands of the transient receptor potential (TRP) channels, capsaicin and icilin: the former activates TPRV1 and the latter TRPA1/TRPM8.

[RESULTS & DISCUSSION]

DRG neurons cultured in the presence of NGF at 100 ng/ml showed spontaneous APs in the cell-attached recording. In 75 % neurons with on-cell firing, transient inward current spikes (named "I_{sp}") were repetitively recorded in the voltage clamp mode at –50 mV in the whole-cell configurations. In contrast, I_{sp} were recorded from only 4.3 % of neurons showing no spontaneous APs in the on-cell mode. These results indicate that I_{sp} relates closely to the spontaneous APs in intact neurons. I_{sp} with stable amplitudes occurred in an all-or-none fashion, and were abolished by TTX, lidocaine and a reduction of extracellular Na^+ in an all-or-none fashion, suggesting that I_{sp} reflect spontaneous firing occurring at loosely voltage-clamped regions. I_{sp} were also observed in the excised outside-out patches, where the kinetics and the sensitivity to the Na^+

channel blockers of I_{sp} resembled those of I_{sp} observed in the whole-cell mode. Spontaneous APs were also recorded in the current clamp mode. Small subthreshold spikes often preceded APs. These results suggest that APs could be generated when localized discharges depolarize the whole-somatic membrane potential to overcome the threshold. TRPV1 antagonists, capsazepine and BCTC, abolished spontaneous APs in the on-cell recordings. Moreover, theses antagonists hyperpolarized the resting membrane potential. These results indicate that the triggering source of APs exists in the somatic membrane itself. Since APs were unaffected by Ca^{2+} removal, Na^{+} influx into neurons thorough TRPV1 could play a key role to trigger the APs in NGF-treated DRG neurons.

In $[Ca^{2+}]_i$ measurements, regardless of the treatment with NGF, about half of the DRG neurons responded to capsaicin and 10% of the neurons responded to icilin. Almost all icilin-responding neurons responded also to capsaicin. $[Ca^{2+}]_i$ fluctuations with large amplitudes were observed in 12 out of 131 NGF-treated neurons. Among these 12 neurons, 10 neurons responded to both capsaicin and icilin. The amplitude of the $[Ca^{2+}]_i$ fluctuations in the NGF-treated neurons responding to both capsaicin and icilin was significantly larger than that in other neurons. These results suggest that NGF acts on neurons expressing both TRPV1 and TRPM8/A1 more effectively and makes

them hyperexcitable. Such neurons are expected to have physiological roles not simply as thermosensors, but also as nociceptors.

[CONCLUSION]

DRG neurons cultured in the presence of NGF show APs that may be resulted from activations of voltage-gated Na^+ channels induced by Na^+ influx through TRPV1 in small fractions of membrane in the absence of any stimuli. Moreover, the amplitude of the $[Ca^{2+}]_i$ fluctuations was significantly larger in neurons that are considered to be nociceptors. These results indicate that NGF acts on the nociceptive DRG neurons and makes them hyperexcitable. If the intrinsic changes in the excitability of the somatic membranes of the nociceptive DRG neurons by NGF observed in this study occurred also *in vivo*, these hyperexcitable DRG neurons may cause unusual pains, such as hyperalgesia and allodynia. The NGF-induced spontaneous activities observed in this study may be one of the underlying mechanisms of the pathogenesis of neuropathic pains.

REFERENCES

Akopian AN, Ruparel NB, Patwardhan A, Hargreaves KM (2008) Cannabinoids desensitize capsaicin and mustard oil responses in sensory neurons via TRPA1 activation. J Neurosci 28:1064-1075.

Akopian AN, Ruparel NB, Jeske NA, Patwardhan A, Hargreaves KM (2009) Role of ionotropic cannabinoid receptors in peripheral antinociception and antihyperalgesia. Trends Pharmacol Sci 30:79-84.

Amir R, Kocsis JD, Devor M (2005) Multiple interacting sites of ectopic spike electrogenesis in primary sensory neurons. J Neurosci 25:2576-2585.

Anand U, Otto W, Casula M, Day N, Davis J, Bountra C, Birch R, Anand P (2006) The effect of neurotrophic factors on morphology, TRPV1 expression and capsaicin responses of cultured human DRG sensory neurons. Neurosci Lett 399:51-56.

Andersson D, Chase H, Bevan S (2004) TRPM8 activation by menthol, icilin, and cold is differentially modulated by intracellular pH. J Neurosci 24:5364-5369.

Andrade E, Luiz A, Ferreira J, Calixto J (2008) Pronociceptive response elicited by TRPA1 receptor activation in mice. Neuroscience 152:511-520.

Babes A, Zorzon D, Reid G (2004) Two populations of cold-sensitive neurons in rat dorsal root ganglia and their modulation by nerve growth factor. Eur J Neurosci 20:2276-2282.

Barbacid M (1994) The Trk family of neurotrophin receptors. J Neurobiol 25:1386-1403.

Bennett D, Averill S, Clary D, Priestley J, McMahon S (1996) Postnatal changes in the expression of the trkA high-affinity NGF receptor in primary sensory

neurons. Eur J Neurosci 8:2204-2208.

Bennett G, Xie Y (1988) A peripheral mononeuropathy in rat that produces disorders of pain sensation like those seen in man. Pain 33:87-107.

Casaccia-Bonnefil P, Gu C, Khursigara G, Chao MV (1999) p75 neurotrophin receptor as a modulator of survival and death decisions. Microsc Res Tech 45:217-224.

Caterina MJ, Schumacher MA, Tominaga M, Rosen TA, Levine JD, Julius D (1997) The capsaicin receptor: a heat-activated ion channel in the pain pathway. Nature 389:816-824.

Chen H, Lamer TJ, Rho RH, Marshall KA, Sitzman BT, Ghazi SM, Brewer RP (2004) Contemporary management of neuropathic pain for the primary care physician. Mayo Clin Proc 79:1533-1545.

Decosterd I, Woolf C (2000) Spared nerve injury: an animal model of persistent peripheral neuropathic pain. Pain 87:149-158.

Devor M, Jänig W, Michaelis M (1994) Modulation of activity in dorsal root ganglion neurons by sympathetic activation in nerve-injured rats. J Neurophysiol 71:38-47.

Eun S, Jung S, Park Y, Kwak J, Kim S, Kim J (2001) Effects of capsaicin on Ca^{2+} release from the intracellular Ca^{2+} stores in the dorsal root ganglion cells of adult rats. Biochem Biophys Res Commun 285:1114-1120.

Fang X, Djouhri L, McMullan S, Berry C, Okuse K, Waxman S, Lawson S (2005) TrkA is expressed in nociceptive neurons and influences electrophysiological properties via $Nav_{1.8}$ expression in rapidly conducting nociceptors. J Neurosci 25:4868-4878.

Fjell J, Cummins TR, Dib-Hajj SD, Fried K, Black JA, Waxman SG (1999) Differential role of GDNF and NGF in the maintenance of two TTX-resistant sodium channels in adult DRG neurons. Brain Res Mol Brain Res 67:267-282.

Galoyan SM, Petruska JC, Mendell LM (2003) Mechanisms of sensitization of the response of single dorsal root ganglion cells from adult rat to noxious heat. Eur J Neurosci 18:535-541.

Hagenacker T, Ledwig D, Büsselberg D (2008) Feedback mechanisms in the regulation of intracellular calcium ($[Ca^{2+}]_i$) in the peripheral nociceptive system: role of TRPV-1 and pain related receptors. Cell Calcium 43:215-227.

Harper A, Lawson S (1985) Electrical properties of rat dorsal root ganglion neurones with different peripheral nerve conduction velocities. J Physiol 359:47-63.

Herzberg U, Eliav E, Dorsey J, Gracely R, Kopin I (1997) NGF involvement in pain induced by chronic constriction injury of the rat sciatic nerve. Neuroreport 8:1613-1618.

Hoheisel U, Mense S, Scherotzke R (1994) Calcitonin gene-related peptide-immunoreactivity in functionally identified primary afferent neurones in the rat. Anat Embryol (Berl) 189:41-49.

Ji R, Samad T, Jin S, Schmoll R, Woolf C (2002) p38 MAPK activation by NGF in primary sensory neurons after inflammation increases TRPV1 levels and maintains heat hyperalgesia. Neuron 36:57-68.

Julius D, Basbaum AI (2001) Molecular mechanisms of nociception. Nature 413:203-210.

Kajander K, Bennett G (1992) Onset of a painful peripheral neuropathy in rat: a partial and differential deafferentation and spontaneous discharge in Aβ and Aδ

primary afferent neurons. J Neurophysiol 68:734-744.

Kajander KC, Wakisaka S, Bennett GJ (1992) Spontaneous discharge originates in the dorsal root ganglion at the onset of a painful peripheral neuropathy in the rat. Neurosci Lett 138:225-228.

Kim S, Chung J (1992) An experimental model for peripheral neuropathy produced by segmental spinal nerve ligation in the rat. Pain 50:355-363.

Kitamura N, Konno A, Kuwahara T, Komagiri Y (2005) Nerve growth factor-induced hyperexcitability of rat sensory neuron in culture. Biomed Res 26:123-130.

Kobayashi K, Fukuoka T, Obata K, Yamanaka H, Dai Y, Tokunaga A, Noguchi K (2005) Distinct expression of TRPM8, TRPA1, and TRPV1 mRNAs in rat primary afferent neurons with Aδ/C-fibers and colocalization with trk receptors. J Comp Neurol 493:596-606.

Komagiri Y, Kitamura N (2003) Effect of intracellular dialysis of ATP on the hyperpolarization-activated cation current in rat dorsal root ganglion neurons. J Neurophysiol 90:2115-2122.

Kárai L, Russell J, Iadarola M, Oláh Z (2004) Vanilloid receptor 1 regulates multiple calcium compartments and contributes to Ca^{2+}-induced Ca^{2+} release in sensory neurons. J Biol Chem 279:16377-16387.

Lawson SN, Crepps BA, Perl ER (1997) Relationship of substance P to afferent characteristics of dorsal root ganglion neurones in guinea-pig. J Physiol 505:177-191.

Lawson SN, Crepps B, Perl ER (2002) Calcitonin gene-related peptide immunoreactivity and afferent receptive properties of dorsal root ganglion

neurones in guinea-pigs. J Physiol 540:989-1002.

Lawson SN, Perry MJ, Prabhakar E, McCarthy PW (1993) Primary sensory neurones: neurofilament, neuropeptides, and conduction velocity. Brain Res Bull 30:239-243.

Levi-Montalcini R, Angeletti PU (1968) Nerve growth factor. Physiol Rev 48:534-569.

Levi-Montalcini R, Skaper SD, Dal Toso R, Petrelli L, Leon A (1996) Nerve growth factor: from neurotrophin to neurokine. Trends Neurosci 19:514-520.

Lewin G, Ritter A, Mendell L (1993) Nerve growth factor-induced hyperalgesia in the neonatal and adult rat. J Neurosci 13:2136-2148.

Lewin GR, Lisney SJ, Mendell LM (1992) Neonatal Anti-NGF Treatment Reduces the Aδ- and C-Fibre Evoked Vasodilator Responses in Rat Skin: Evidence That Nociceptor Afferents Mediate Antidromic Vasodilatation. Eur J Neurosci 4:1213-1218.

Liu M, Liu M, Magoulas C, Priestley J, Willmott N (2003) Versatile regulation of cytosolic Ca^{2+} by vanilloid receptor I in rat dorsal root ganglion neurons. J Biol Chem 278:5462-5472.

Luo W, Wickramasinghe SR, Savitt JM, Griffin JW, Dawson TM, Ginty DD (2007) A hierarchical NGF signaling cascade controls Ret-dependent and Ret-independent events during development of nonpeptidergic DRG neurons. Neuron 54:739-754.

Matzner O, Devor M (1994) Hyperexcitability at sites of nerve injury depends on voltage-sensitive Na^{+} channels. J Neurophysiol 72:349-359.

McKemy D, Neuhausser W, Julius D (2002a) Identification of a cold receptor

reveals a general role for TRP channels in thermosensation. Nature 416:52-58.

McKemy DD, Neuhausser WM, Julius D (2002b) Identification of a cold receptor reveals a general role for TRP channels in thermosensation. Nature 416:52-58.

Millan MJ (1999) The induction of pain: an integrative review. Prog Neurobiol 57:1-164.

Minke B, Cook B (2002) TRP channel proteins and signal transduction. Physiol Rev 82:429-472.

Montell C (2001) An end in sight to a long TRP. Neuron 30:3-5.

Mu X, Silos-Santiago I, Carroll S, Snider W (1993) Neurotrophin receptor genes are expressed in distinct patterns in developing dorsal root ganglia. J Neurosci 13:4029-4041.

Namaka M, Gramlich CR, Ruhlen D, Melanson M, Sutton I, Major J (2004) A treatment algorithm for neuropathic pain. Clin Ther 26:951-979.

Ozaki Y, Kitamura N, Tsutsumi A, Dayanithi G, Shibuya I (2009) NGF-induced hyperexcitability causes spontaneous fluctuations of intracellular Ca^{2+} in rat nociceptive dorsal root ganglion neurons. Cell Calcium 45:209-215.

Patapoutian A, Tate S, Woolf CJ (2009) Transient receptor potential channels: targeting pain at the source. Nat Rev Drug Discov 8:55-68.

Patapoutian A, Peier AM, Story GM, Viswanath V (2003) ThermoTRP channels and beyond: mechanisms of temperature sensation. Nat Rev Neurosci 4:529-539.

Peier AM, Moqrich A, Hergarden AC, Reeve AJ, Andersson DA, Story GM, Earley TJ, Dragoni I, McIntyre P, Bevan S, Patapoutian A (2002) A TRP channel that senses cold stimuli and menthol. Cell 108:705-715.

Pezet S, McMahon S (2006) Neurotrophins: mediators and modulators of pain. Annu

Rev Neurosci 29:507-538.

Price T, Louria M, Candelario-Soto D, Dussor G, Jeske N, Patwardhan A, Diogenes A, Trott A, Hargreaves K, Flores C (2005) Treatment of trigeminal ganglion neurons in vitro with NGF, GDNF or BDNF: effects on neuronal survival, neurochemical properties and TRPV1-mediated neuropeptide secretion. BMC Neurosci 6:4.

Ramsey IS, Delling M, Clapham DE (2006) An introduction to TRP channels. Annu Rev Physiol 68:619-647.

Ritter AM, Lewin GR, Kremer NE, Mendell LM (1991) Requirement for nerve growth factor in the development of myelinated nociceptors in vivo. Nature 350:500-502.

Ruparel NB, Patwardhan AM, Akopian AN, Hargreaves KM (2008) Homologous and heterologous desensitization of capsaicin and mustard oil responses utilize different cellular pathways in nociceptors. Pain 135:271-279.

Sebert M, Shooter E (1993) Expression of mRNA for neurotrophic factors and their receptors in the rat dorsal root ganglion and sciatic nerve following nerve injury. J Neurosci Res 36:357-367.

Seltzer Z, Dubner R, Shir Y (1990) A novel behavioral model of neuropathic pain disorders produced in rats by partial sciatic nerve injury. Pain 43:205-218.

Shen H, Chung J, Chung K (1999) Expression of neurotrophin mRNAs in the dorsal root ganglion after spinal nerve injury. Brain Res Mol Brain Res 64:186-192.

Shu X, Mendell L (1999a) Nerve growth factor acutely sensitizes the response of adult rat sensory neurons to capsaicin. Neurosci Lett 274:159-162.

Shu X, Mendell LM (2001) Acute sensitization by NGF of the response of

small-diameter sensory neurons to capsaicin. J Neurophysiol 86:2931-2938.

Shu XQ, Mendell LM (1999b) Neurotrophins and hyperalgesia. Proc Natl Acad Sci U S A 96:7693-7696.

Song XJ, Zhang JM, Hu SJ, LaMotte RH (2003) Somata of nerve-injured sensory neurons exhibit enhanced responses to inflammatory mediators. Pain 104:701-709.

Story G, Peier A, Reeve A, Eid S, Mosbacher J, Hricik T, Earley T, Hergarden A, Andersson D, Hwang S, McIntyre P, Jegla T, Bevan S, Patapoutian A (2003) ANKTM1, a TRP-like channel expressed in nociceptive neurons, is activated by cold temperatures. Cell 112:819-829.

Verge V, Richardson P, Benoit R, Riopelle R (1989) Histochemical characterization of sensory neurons with high-affinity receptors for nerve growth factor. J Neurocytol 18:583-591.

Verge V, Richardson P, Wiesenfeld-Hallin Z, Hökfelt T (1995) Differential influence of nerve growth factor on neuropeptide expression in vivo: a novel role in peptide suppression in adult sensory neurons. J Neurosci 15:2081-2096.

Wall P, Devor M, Inbal R, Scadding J, Schonfeld D, Seltzer Z, Tomkiewicz M (1979) Autotomy following peripheral nerve lesions: experimental anaesthesia dolorosa. Pain 7:103-111.

Wiesmann C, de Vos AM (2001) Nerve growth factor: structure and function. Cell Mol Life Sci 58:748-759.

Winkelstein B, Rutkowski M, Weinstein J, DeLeo J (2001) Quantification of neural tissue injury in a rat radiculopathy model: comparison of local deformation, behavioral outcomes, and spinal cytokine mRNA for two surgeons. J Neurosci

Methods 111:49-57.

Winter J, Forbes CA, Sternberg J, Lindsay RM (1988) Nerve growth factor (NGF) regulates adult rat cultured dorsal root ganglion neuron responses to the excitotoxin capsaicin. Neuron 1:973-981.